INTERNATIONAL ATOMIC ENERGY AGENCY
UNITED NATIONS EDUCATIONAL, SCIENTIFIC AND CULTURAL ORGANIZATION

INTERNATIONAL CENTRE FOR THEORETICAL PHYSICS
34100 TRIESTE (ITALY) - P.O.B. 586 - MIRAMARE - STRADA COSTIERA 11 - TELEPHONES: 224281/2/3/4/5/6
CABLE: CENTRATOM - TELEX 460392 - 1

SMR/388 - 18

SPRING COLLEGE IN MATERIALS SCIENCE
ON
"CERAMICS AND COMPOSITE MATERIALS"
(17 April - 26 May 1989)

CREEP AND DEFORMATION

G.S. DAEHN
Department of Materials Science and Engineering
The Ohio State University
116 W. 19th Avenue
Columbus, Ohio 43210

Creep and Deformation

Lecture notes prepared for:
Spring College in Materials Science
"Ceramics and Composite Materials"
International Center for Theoretical Physics
Trieste, Italy

2 - 5 May 1989

Lecturer: Glenn S. Daehn
Assistant Professor
Department of Materials Science and Engineering
The Ohio State University
116 W. 19th Avenue
Columbus, Ohio 43210

Outline of Lecture Series

O. Overview

A. Fundamentals of Creep and Deformation
- Deformation at low and high temperature
- Experimental techniques
- Experimental results and data presentation

B. Mechanistics of Creep Deformation
- Diffusional Creep
- Dislocation Based Creep
- Class I Solid Solutions
- Grain Boundary Sliding
- Dispersion strengthened materials
- The Big Picture -- Maps and the Dorn Equation

C. Creep in Specific Systems
- Comparison between metallic and ceramic creep
- Superplasticity
  - basic principles
  - zirconia

D. High Temperature Cavitation and Crack Growth
- Types of Damage
- Multiaxial Stress States
- Crack Growth at elevated Temperature

E. Effects of Internal Stresses
- Experimental Observations
- Phase changes
- Changing Temperature
  - Whisker reinforced composites
  - Fiber reinforced composites

F. Creep Resistant Materials

General References:

W. D. Kingery, H. K. Bowen and D. R. Uhlmann: *Introduction to Ceramics*, John Wiley and Sons, 1976.

W. R. Cannon and T. G. Langdon: "Review -- Creep of Ceramics, Part I Mecanical Characteristics, *J. Mat. Sci*, **18**, pp. 1-50, (1983).

J. P. Porier, *Creep of Crystals*, Cambridge University Press, 1987.

R. W. Evans and B. Wilshire, *Creep of Metals and Alloys*, The Institute of Metals, 1985.

O. D. Sherby and P. Burke, "Mechanical Behavior of Crystalline Solids at Elevated Temperature", *Progress in Materials Science*, **13**, 324 (1968).

A. G. Evans and T. G. Langdon, "Structural Ceramics", *Progress in Materials Science*, **21**, 171 (1976).

R. Raj (ed.): "Flow and Fracture at Elevated Temperatures", American Society for Metals, Metals Park, Ohio, 1985. In particular see the paper "Mechanisims of Time-Dependent Flow and Fracture of Meals" by W. D. Nix and J. C. Gibeling.

R. W. Hertzberg, *Deformation and Fracture of Engineering Materials*, Third Edition, Chapter Five, Wiley, 1989.

O. Overview

This is quite an expansive topic.
Most creep phenomena are still not well understood.
There is a better understanding of metallic than ceramic creep (more data,too).

For these reasons this presentation will have a limits and emphasis as follows:

- Most illustrations of mechanistics will come from metals and be extended to ceramics.
- Only the better accepted theories of will be presented.
- Areas of controversy will be noted.
- Experimental observations/correlations and applications will be emphasized.
- This presentation will deal with "elevated temperature deformation" only

(Elevated temperature refers to $T>0.35T_m$ in metals, and $T>0.45T_m$ for ceramics)

A. Fundamentals of Creep and Deformation

Creep Testing.

The simplest method of creep testing is to simply stress a sample in tension (via. a fixed load, or a load which decreases with strain to approximate constant stress) and monitor the sample elongation as a function of time. A gage is usually affixed to the sample for this.

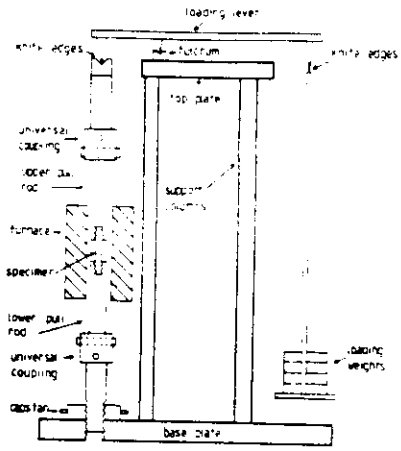

Figure A. Creep test schematic (From Evans and Wilshire).

Deformation at low and high temperature

Again, This presentation will deal with "elevated temperature deformation" only. For our purposes, elevated temperature refers to $T>0.35T_m$ in metals, and $T>0.45T_m$ for ceramics.

Let's Examine why we draw this distinction. This temperature range is empirically found to be the range in which self diffusion begins to operate at a significant rate. This changes the both the mechanical response of solids and the structure which is developed after deformation. Specifically:

A) Metals

Considering the strain-time curve, at low temperatures $T<0.4\ T_m$, creep rate continually decreases with strain. This is known as logarithmic creep. Above $0.4\ T_m$, there are often three distinct regions in the time elongation plot:

Primary creep - equivalent to strain hardening,

Steady state creep - hardening and recovery balance,

Tertiary creep - cracks and voids weaken the structure.

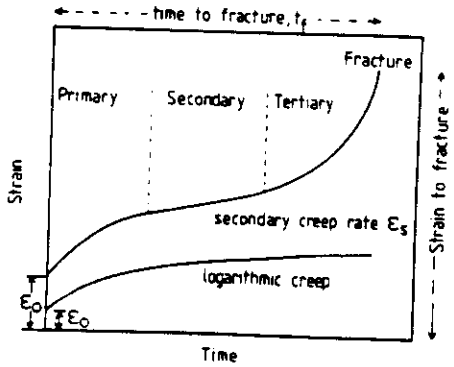

Figure B. Schematics of logarithmic and high temperature creep.

The structures which develop also differ at low vs. high temperature. at low temperatures "cell formation" dominates. Whereas at elevated temperature "subgrain formation" typically dominates. Cells are thick and disordered regions of high

dislocation density. Cell size decreases and dislocation density increases as strain accumulates. If $T>0.4T_m$ the subgrain size and dislocation density are nearly determined by the applied stress only.

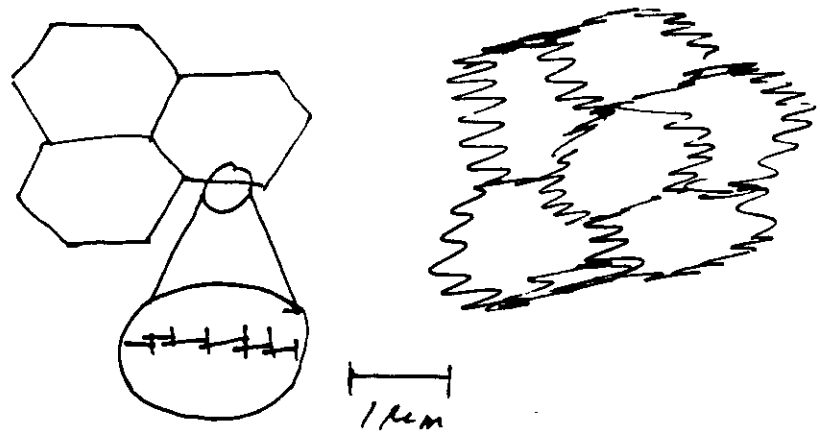

Subgrain Structure Cell Structure

Figure C. Schematic representation of cell and subgrain microstructures

B) Ceramics

The above comments seem to generally hold for ceramics as well, however 1) dislocation motion is often very difficult below $0.4T_m$ and, 2) it is often very difficult to propagate slip across grain boundaries. Therefore, in ceramics fracture often hinders the study of significant plastic deformation of ceramics at relatively low temperatures. But, primary, steady-state and tertiary creep curves have often been observed in ceramics, and subgrains have also been observed after dislocation-creep in ceramics.

For reference, the kinds of temperatures required for the onset of creep:

Metal	$0.35T_m$	Ceramic	$0.45T_m$
Aluminum	53 C	Alumina	772 C
Iron	221 C	Silicon carbide	1126 C
Titanium	238 C	Diamond	1527 C
Tungsten	919 C		

Experimental techniques

Test Methods and Advantages

The text by Evans and Wilshire treats the instrumentation for creep testing in uniaxial compression and tension quite extensively. Here, the test methods available and correlations between data generated by various test methods will be emphasized. Generally, in designing a test the experimenter must specify three things:

1) The variable controlled

In all cases either stress or strain must be controlled, while the other is measured. In creep testing the stress is typically controlled. However, it is perfectly acceptable to use fix the displacement rate and measure load (as is common in low temperature testing).

Equivalent data is usually obtained, but it is often difficult to control low rates of displacement accurately.

2) How that variable is controlled

If stress is controlled in tension it is simplest to apply a fixed load, then the stress will increase as strain accumulates. However, a number of schemes are available to approximate constant stress (most notably the Andrade arm). In strain control, computer-interfaced testing machines can approximate constant true strain rate conditions. Constant stress, or strain-rate is preferred for theoretical studies but these conditions are more difficult to obtain.

3) Test specimen geometry and stress state (Experimental Techniques)

A number of testing methods are available. Each with advantages and disadvantages:

- Tensile - most typical, not often applicable to ceramics.
- Compression - simple and fundamental, friction problems at high strain.
- Torsion - good for work at high plastic strains, strain gradient if solid cylinder.
- 4-point bending - common in ceramics, somewhat difficult to analyze.
- Biaxial tension - pressure under diaphragm, common with superplastic alloys.
- Notched tensile - used for studies on damage accumulation in creep.
- Impression creep - good for inhomogeneous structure, hard to analyze.

Equivalency of Test Methods

In order to compare results obtained in different stress states, we must accept a plastic flow law. The two most common are:

1) Tresca Criterion

if $\tau_{applied} = \tau_{critical}$ then plastic flow is initiated, or at yield

$$\frac{\sigma_{max} - \sigma_{min}}{2} = \tau_{critical}$$ where τ_{crit} is one half the uniaxial flow stress.

2) vonMises Criterion

The three principal stresses are defined as σ_1, σ_2 and σ_3. σ_y is the yield strength:

at the onset of plastic flow $$\sigma_y = \frac{1}{\sqrt{2}}\left((\sigma_1 - \sigma_2)^2 + (\sigma_1 - \sigma_3)^2 + (\sigma_2 - \sigma_3)^2\right)^{\frac{1}{2}}$$

First, as an example let's examine these equations in for strain-rate insensitive materials with a tensile yield stress arbitrarily set at 100 MPa. Consider four loading conditions:

	σ_1	σ_2	σ_3
Tension	applied stress	0	0
Compression	0	0	-(applied stress)
Simple shear	applied shear stress	0	– (applied shear stress)
biaxial tension	applied stress	applied stress	0

The measured yield stresses will be:

	Tresca	vonMises
Tensile	σ=100 MPa	σ=100 MPa
Compression	σ=100 MPa	σ=100 MPa
Simple shear	τ=50 MPa	τ=57.7 MPa (note yield varies 15%)
Biaxial tension	σ=100 MPa	σ=100 MPa

In creep, defined yield stresses do not exist! Therefore we generalize these ideas to give effective stresses, $\bar{\sigma}$, effective strains, $\bar{\varepsilon}$,and effective strain rates, $\dot{\bar{\varepsilon}}$. Effective stresses are developed similarly to the above discussion:

For Tresca: $\bar{\sigma} = 2\tau_{max}$

For vonMises: $$\bar{\sigma} = \frac{1}{\sqrt{2}}\left((\sigma_1 - \sigma_2)^2 + (\sigma_1 - \sigma_3)^2 + (\sigma_2 - \sigma_3)^2\right)^{\frac{1}{2}}$$

also, since plastic work should be independent of definition, (i.e.), effective strains can be defined as:

Tresca: $$\bar{\varepsilon} = \frac{\gamma}{2}$$

vonMises: $$\bar{\varepsilon} = \left[\tfrac{2}{3}(\varepsilon_1^2 + \varepsilon_2^2 + \varepsilon_3^2)\right]^{\frac{1}{2}}$$ (for proportional strain path only!)

Now for any reasonably isotropic material (at fixed structure and temperature) we can use the above relationships and develop a function: $\dot{\bar{\varepsilon}} = f(\bar{\sigma})$. This function is independent of the geometry of the test, thus the most convenient test can be run and the results may be applied to another geometry. In uniaxial testing the actual and effective quantities are the same.

For example in shear, or torsion testing:

	Tresca	vonMises
$\bar{\sigma}$	2τ	$\sqrt{3}\ \tau$
$\dot{\bar{\varepsilon}}$	$\frac{\dot{\gamma}}{2}$	$\frac{\dot{\gamma}}{\sqrt{3}}$

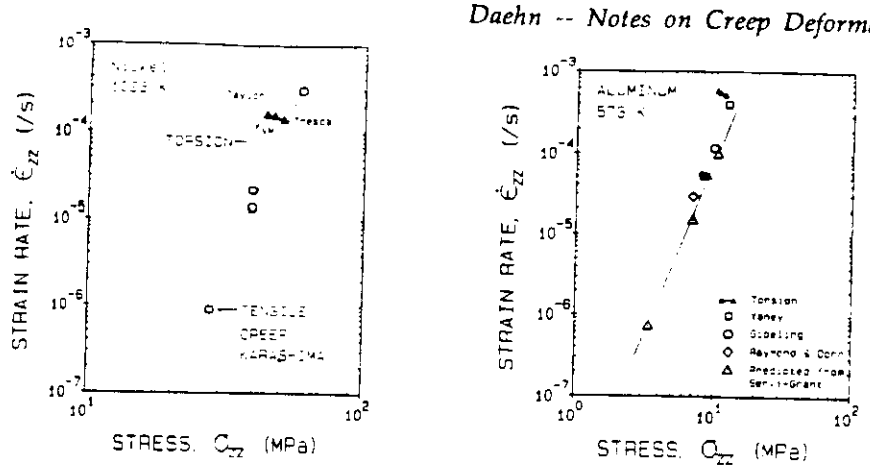

*Figure D. The application of these concepts in testing is illustrated in this figure from D. A. Hughes and W. D. Nix, Met. Trans., **19A**, p. 3023 (1988).*

These ideas can be extended to determine general strains under general states of stress. The Levy-vonMises, or Prandl-Reuss Equations treat these kinds of problems. See a text on continuum mechanics for details.

Experimental results and data presentation

A) Effect of Temperature and Strain Rate

The early works of Zener and Holoman[1] suggested that increased strain rate and decreased temperature could be effectively "traded". In this framework the flow stress of a plastic solid could be expressed as:

$$\sigma = \Phi(\varepsilon, Z)$$

$$\text{where,} \quad Z \equiv \dot{\varepsilon} \exp\left(\frac{\Delta H}{RT}\right)$$

This concept was supported by data from Tozerra, Sherby and Dorn[2] who found that at the same values of Z, identical stress-strain curves could be obtained in polycrystalline high purity aluminum.

[1] *J. Appl. Phys.*, **15**, p.15 (1944).
[2] *Trans ASM*, **49**, p. 173 (1957).

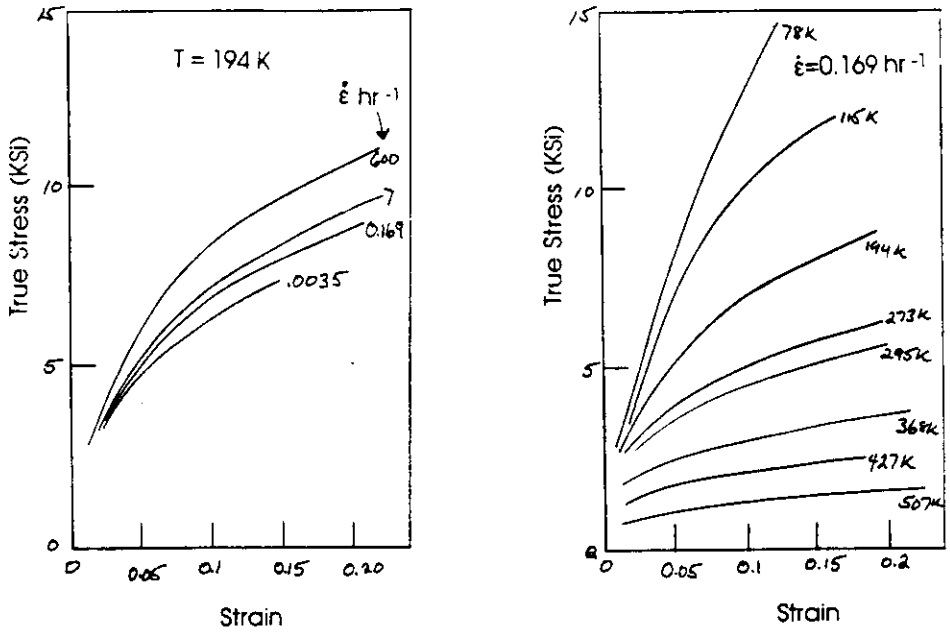

Figure E. Stress strain curves from high purity polycrystalline alumina) Effect of strain rate at a fixed temperature of 194K b) Effect of Temperature at fixed a fixed strain rate of 0.169 hrs^{-1} (data from Trozera, Sherby and Dorn).

One may use a similar approach with data obtained from conventional creep tests. This was illustrated in the review by Sherby and Burke, and is the basis for the Orr, Sherby, Dorn approach to life prediction.

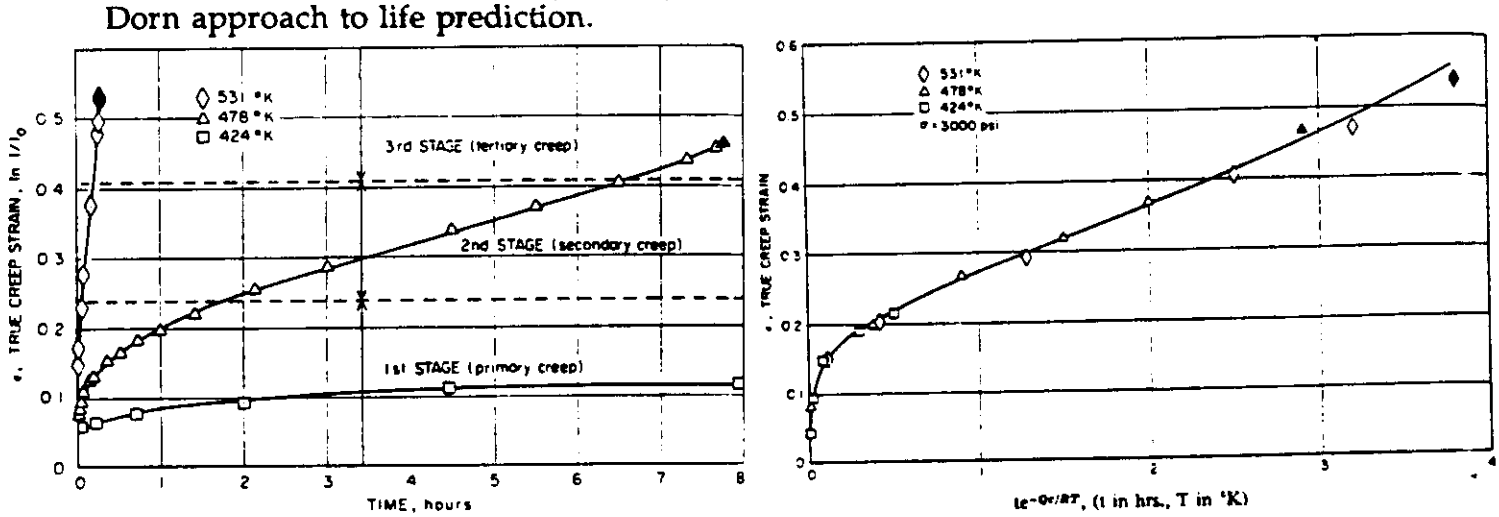

Figure F. Creep curves from high purity aluminum tested at a stress of 3000 psi. a) raw creep data, b) correlated by the parameter Θ=(t exp(-Q/RT)) where Q=34Kcal/mol. From Sherby and Burke.

The key concept shown in these two analyses is that **decreased strain rate (or increased available time) is equivalent to increased temperature. This suggests plastic** deformation may be a thermally activated process (similar to chemical reactions). This will be examined further.

B) Activation Energies

One way in which the activation energy in the Zener-Holoman parameter can be evaluated without comparing creep curves is by performing tests in which the temperature is abruptly changed during a creep test. Thus, strain, stress and microstructure will be held nearly constant[1]. Two conclusions have come out of this kind of work: 1) Q is independent of creep strain and 2) above $0.6T_m$ Q was independent of temperature and approximately equal to the activation energy for self diffusion.

In principle, temperature change tests and the technique of correlating stress-strain or strain-time curves to a particular Zener-Holoman parameter could be used to determine the activation energies for creep. However, flow under steady-state conditions has been emphasized by many research teams. Thus, one may extend the Zener-Holoman approach and say:

$$\dot{\epsilon}_{ss} = f(\sigma_f)\exp\left(\frac{-Q_c}{RT}\right)$$

Thus, if stress is held constant, the activation energy for plastic deformation may be obtained in a straightforward way, as illustrated below:

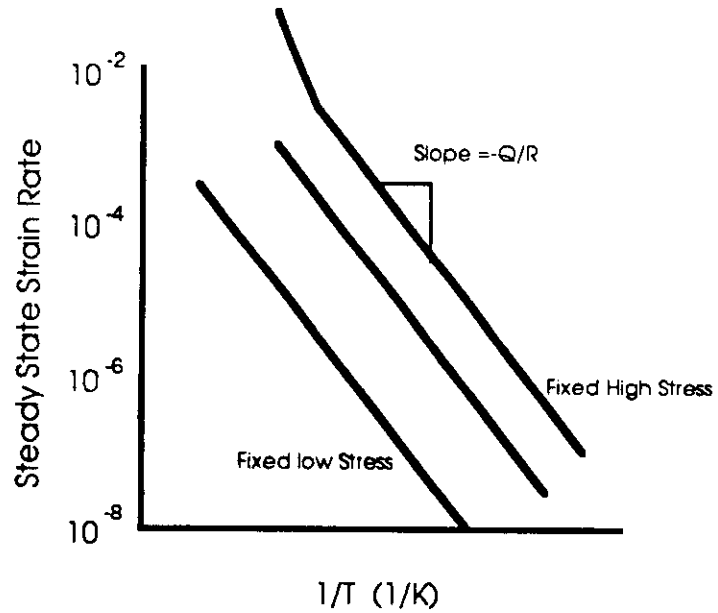

Figure H. Schematic illustration of the graphical technique for finding the activation energy for creep.

Using the techniques outlined above one may plot the activation energies for plastic deformation as a function of temperature. Examples are shown below for pure polycrystalline aluminum and sodium chloride. These both show that at high homologous temperature the activation energy becomes approximately equal to that for self diffusion of aluminum and chlorine ions.

---

[1] see: Landon, Lytton, Shepard and Dorn *Trans ASM*, **51**, 900 (1959), and Conrad *J Metals*, July 1964 p. 582.

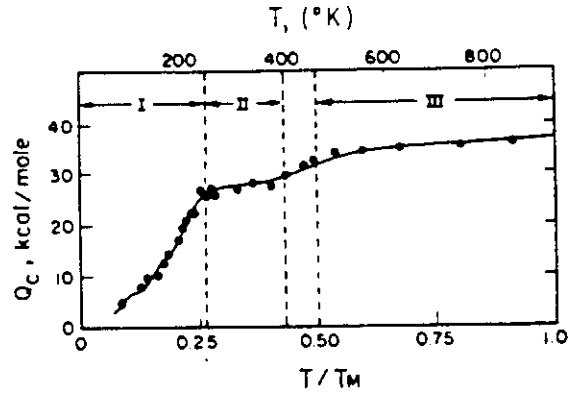

Figure I. Activation energy of pure polycrystalline aluminum as a function of temperature (from Sherby and Burke)

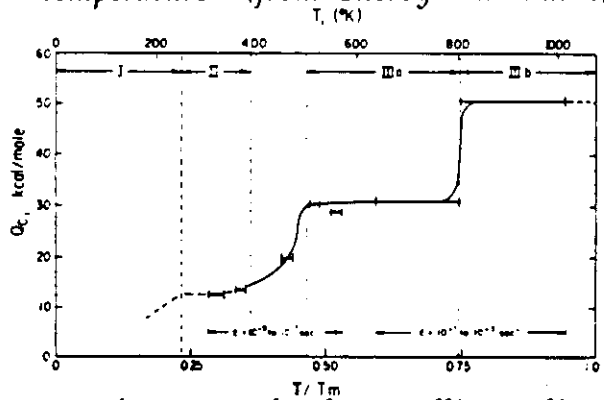

Figure J. Activation Energy for creep of polycrystalline sodium chloride as a function of temperature (from Sherby and Burke).

C) The stress dependence of creep rate

The traditional method of displaying the relationship between the steady state creep rate and the applied stress by plotting each quantity on a logarithmic scale. The relationships are typically linear on these axes. Based on these, the stress exponent, n, and the strain rate sensitivity exponent, m, are defined as:

These quantities have fundamental meaning and the methods for determining them are illustrated below.

$$n = \left(\frac{\partial \ln \dot{\varepsilon}}{\partial \ln \sigma}\right)$$

$$m = \frac{1}{n} = \left(\frac{\partial \ln \sigma}{\partial \ln \dot{\varepsilon}}\right)$$

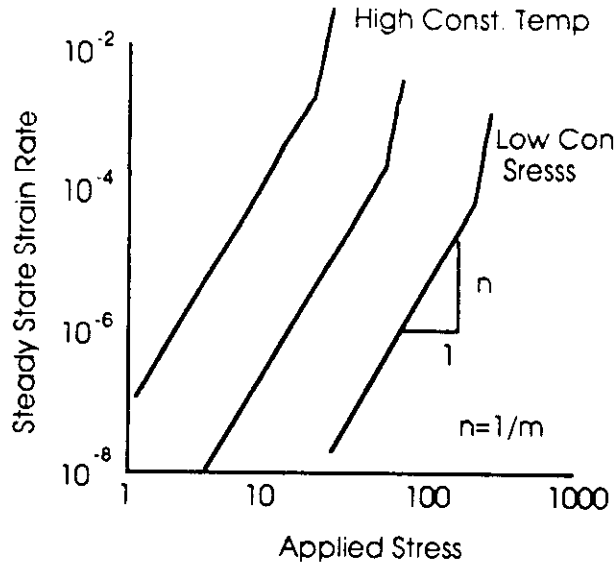

Figure K. Typical relationships between applied stress and steady state strain rate for creeping solids.

An Exercise:

Samples for elevated temperature tensile testing were all made from a single heat of an annealed single phase metal. These samples were tested under controlled true-strain-rate conditions, at three temperatures and three strain rates. In all cases, after a few percent strain, a well defined steady state flow stress was observed. This flow stress as at each temperature and strain rate are shown below.

	Flow Stress (MPa) Temperature (°C)		
Strain Rate	400	450	500
1E-4	20.3	14.6	11.0
5E-4	34.7	25.0	18.7
1E-3	43.7	31.4	23.6

Based on these data what is the equation for steady state creep and the activation energy for creep in this metal?

Answers: $n=3$, $Q_c=75KJ/mol$

B. Mechanistics of Creep Deformation

In this section we will examine the commonly observed mechanisms for creep in simple systems. From these somewhat phenomenological models of creep deformation,

It will be suggested that the activation energy, stress exponent and transient behavior can be used to gain fundamental insight to the deformation process.

The Evidence for Diffusional Control in Creep

It is widely accepted that the deformation rates of nearly all solids, above $0.5T_m$ is controlled by self diffusion. The theoretical explanations for this is covered in the following sections. The Experimental evidence is as follows:

1) Based on tests referenced above, it is found that the activation energy for creep is not a function of plastic strain.

2) Based on the same kinds of tests, it is found that above $0.6T_m$ there seems to be a plateau in the activation energy. These plateau activation energies for creep, Q_c, can be compared to the activation energy for self diffusion, Q_d, for a number of metals. This is shown in Figure L. This same kind of correlation is illustrated in Figure M for ceramic materials. In this case Q_c is compared to the activation energy for the slowest moving species.

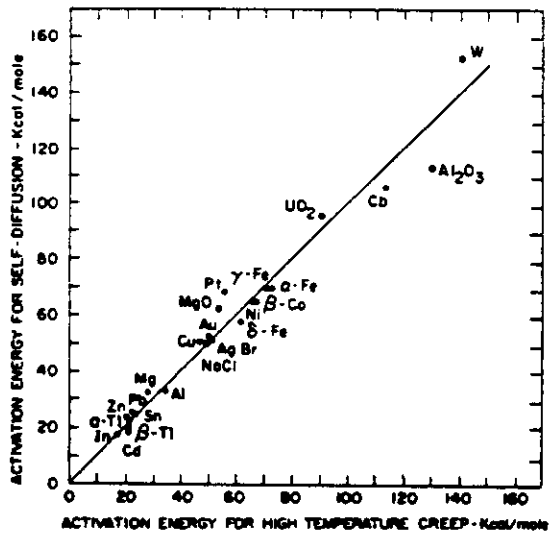

Figure L. Activation Energy for creep at 0,5 T_m, Q_c compared to the activation energy for self diffusion in a number of pure polycrystalline metals. (from Sherby and Burke)

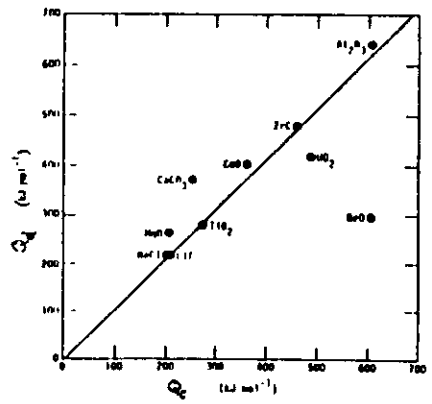

Figure M. Comparison of Q_C and Q_D of the slowest moving species for a number of polycrystalline ceramic materials. (From Langdon and Evans).

3) The pressure dependence of creep and deformation can both be expressed by an activation volume concept. Weertman[1] has used a similar plot, Figure N, to show that the activation volumes for creep and self-diffusion are very similar for a number of metals and compounds.

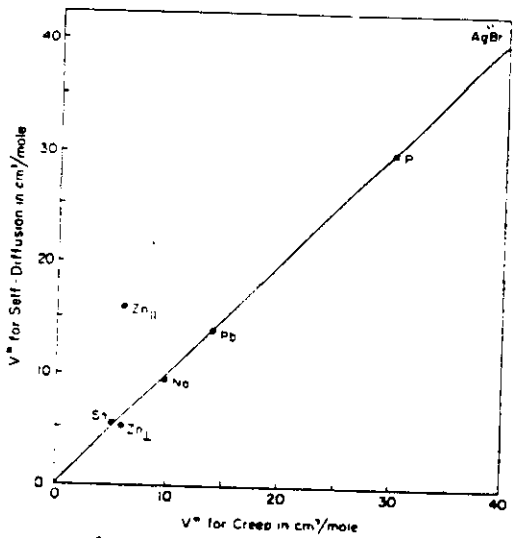

Figure N. Activation volumes for creep and self diffusion for a number of single-phase solids. (from Weertman)

4) Effects of added solutes often have identical effects on the creep rates and self-diffusion rate. This is illustrated in Figure O. The same behavior has been observed in many ceramic systems, as shall be discussed later. Similarly, phase transitions often produce parallel changes in creep rate and diffusion rate.

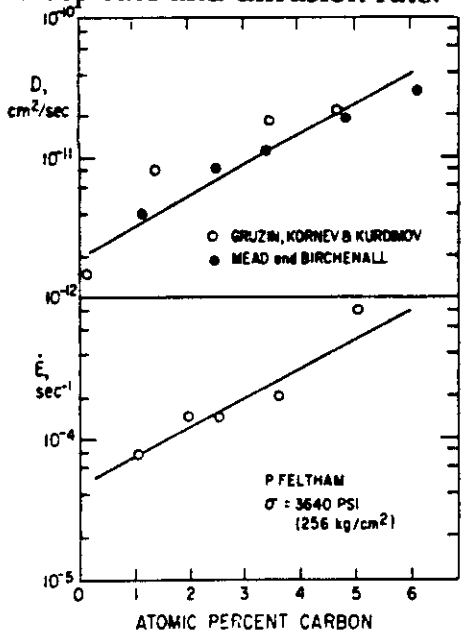

Figure O. Effect of carbon content on the self diffusion rate, and creep rate in austenitic iron at 1000° C. (from Sherby and Burke)

[1] *Trans. ASM*, 61, 681 (1968)

Diffusional Creep

Creep by purely diffusional mechanisms dominates at relatively low stresses ($\sigma/E<10^5$) and high temperatures ($T>0.9T_m$). The mechanistics can be easily understood by first recognizing that a grain boundary cannot withstand shearing forces at elevated temperature. Thus, the stress state within each grain is not uniform. Specifically a tensile stress will act on boundaries perpendicular to the tensile stress axis and vice-versa. By the convention in Figure O*, the energy barrier to creating a vacancy on "A" type boundaries will be ($Q_f-\sigma b^3$). While on "B" type boundaries the energy barrier will be ($Q_f+\sigma b^3$). Thus, there will be a higher concentration of vacancies on "A" boundaries than on "B" boundaries, and a vacancy flux will be set up in accord with Fick's laws.

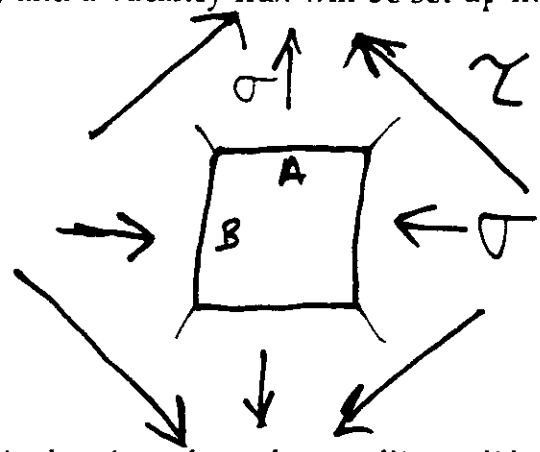

Figure O. Schematic drawing of a polycrystalline solid under a state of pure shear stress.*

Note that the vacancy flux will travel both through the bulk and along grain boundaries and these will contribute independently to the strain in the polycrystal. In the case where bulk diffusion is dominant, Nabarro[1] and Herring[2] have determined that the strain rate of the polycrystal is:

$$\dot{\varepsilon} = 0.7B\frac{D_l b}{kT}\left(\frac{b}{G}\right)^2\sigma$$

Where: G is the grain diameter
B is a geometric constant which is typically between 12 and 40

Coble[3] has analyzed the situation in which the flow of vacancies takes place along grain boundaries. For the case of creep in uniaxial tension, the creep rate was calculated as:

$$\dot{\varepsilon} = 33.4B\frac{D_{gb} b}{kT}\left(\frac{d_{gb}}{b}\right)\left(\frac{b}{G}\right)^3\sigma$$

Here, d_{gb} is the width of the grain boundary region.

---

1 F. R. N. Nabarro: *Rpt. Conf. Str. Sol.*, p. 75, The Physical Society, London (1948).
2 C. Herring: *J. Appl. Phys.*, **21**, 437 (1950).
3 R. L. Coble: *J. Appl. Phys*, **34** 1679 (1963).

There is good evidence for the existence of both of these processes, both from comparison of experiment to theory and metallographic observations.

Notes on diffusional creep:

• Coble and Nabarro-Herring creep are independent processes. Thus, the creep rate of the solid is equal to the sum of the above equations

• Smaller grain sizes and lower temperatures favor Coble creep over Nabarro-Herring Creep. This can be understood by consideration of Figure P.

• There are a number of morphological features of diffusional creep which are worthy of note. If the grains are elongated in the tensile direction, the effective diffusion length for diffusional creep is increased and the creep rate decreases. Also, diffusional flow changes the shape of individual crystals. If the aggregate is to fill space, concurrent grain boundary sliding is required.

• The above represent continuum analyses of diffusional flow (i.e. grain boundaries are perfect sources and sinks for vacancies). Artz, *et. al.*[1] have shown second-order effects (such as small numbers of sources and sinks, and solute-limited dislocation mobility) can be important in many circumstances.

• There is another mechanism, Harper-Dorn[2] creep, which is active at high homologous temperature and low stress. This also shows strain rate being proportional to stress, and a creep activation energy approximately equal to that for lattice self diffusion. However, experimentally it has been shown that creep rate in H-D creep is independent of grain size. The mechanistics of this process are still very much in debate[3].

↓

At dislocation density, ρ, is independent of Stress

[1] E. Artz, M. F. Ashby and R. A. Verrall: *Acta Met*, **31**, 1977 (1983).

[2] J. G. Harper and J. E. Dorn: *Acta Metall.*, **5**, (1958).

[3] For example see: J. Blacic and J. Weertman: *Geophys Res. Lett.*, **11**, 117, (1984), F. A. Mohammed and T. J. Ginter: *Acta Metall.*, **30**, (1982) or O. A. Ruano, J. Wadsworth and O. D. Sherby: *Acta Metall.*, **36**, 1117 (1988).

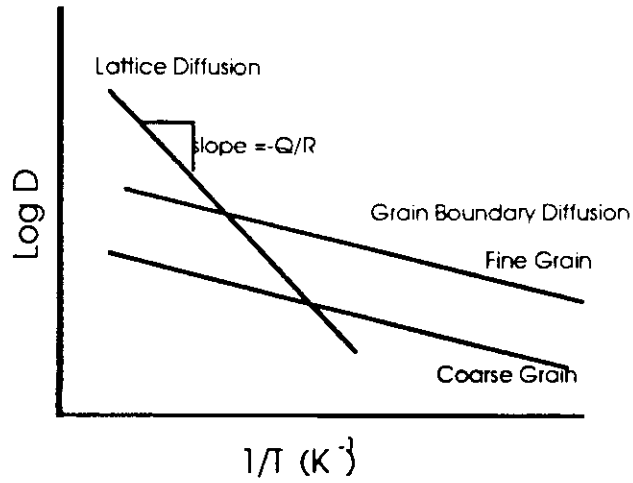

Figure P. Schematic illustration of the effect of temperature and grain size on diffusion and diffusional creep rates.

Application to Ceramics

Diffusional flow is an important deformation mechanism in ceramic materials. In order to avoid local compositional differences two or more species must diffuse in a coupled manner. In these cases the rate of diffusional creep is determined by **the movement of the slowest species along its fastest diffusional path.** The review by Evans and Langdon discusses this in some depth.

Dislocation Based Creep (Pure metals)

At lower temperatures and higher stresses deformation occurs via the movement of dislocations through the lattice. "Simple" dislocation creep of pure metals is probably the most commonly observed and theoretically most complicated and debated phenomenon in creep.

A) Experimental Observations

It is commonly observed that the stress exponent for creep in pure metals is approximately 5. If the strain rate is normalized to the lattice diffusion coefficient, the stress v. normalized strain-rate behavior for a single metal will collapse to one curve. Three regions can be seen (Figure Q): at low stress, diffusional flow will dominate; at intermediate stress, n=5, power law creep is observed; and at very high stresses, power-law break down is observed[1]. This high-stress behavior will not be discussed further.

[1] F. Garafolo: *Trans ASM-AIME*, **227**, 351 (1963).

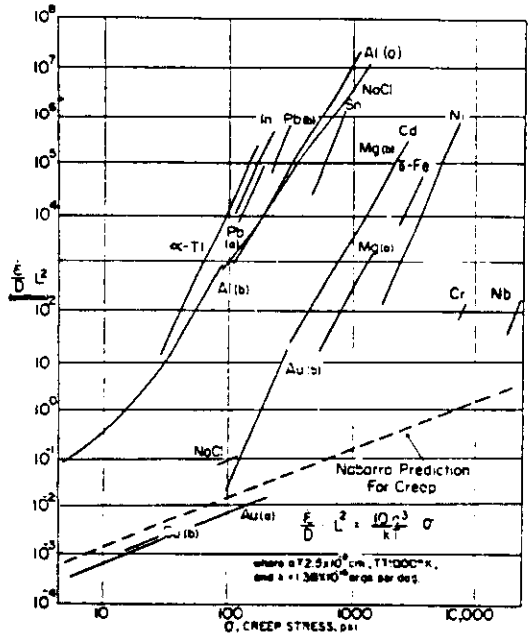

Figure Q. Stress v. normalized strain-rate behavior for a number of pure metals above 0.6 T_M (From Sherby and Burke).

In the intermediate stress range a relationship can be written:

$$\sigma = \sqrt[5]{\frac{\dot{\varepsilon}}{D_L}}\,K(M)$$

Here K(M) is some function of the physical properties of the metal. Let's examine this further by examining K(M) with the other term fixed. Figure R shows the relationship between flow stress with ($\dot{\varepsilon}/D_L$) set at 10^7 cm^{-2} and the elastic modulus.

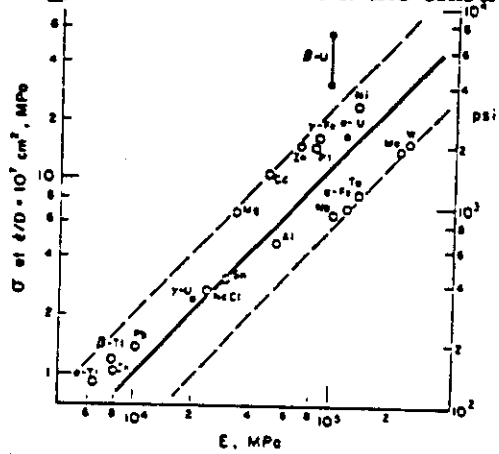

Figure R. Relationship between the flow stress (at fixed normalized strain rate) and elastic modulus. This shows that the flow stress at any strain rate is primarily a function of elastic modulus, when tested at a temperature at which atom mobility is the same. (from Sherby and Miller[1]).

[1] O. D. Sherby and A. K. Miller: *J. Eng. Mat. and Tech.*, **101**, 387 (1979).

Based on this we can develop a first-order equation for the power-law creep of pure metals as:

$$\dot{\varepsilon}_{ss} = \frac{10^{11}}{b} D_L \left(\frac{\sigma}{E}\right)^5$$

Note that now we have two temperature dependent terms D and E. This now means that if the activation energy for creep is to be evaluated, any experiments should be carried out at a constant normalized stress (i.e. σ/E). If tests are carried out at constant stress, at various temperatures, an anomalously high modulus will result. The corrected modulus can be calculated as:

$$Q_c^{True} = Q_c^{Apparent} + \frac{nRT^2}{E}\left(\frac{dE}{dT}\right)$$

Note that in this expression, the final term is always negative.

Elastic modulus clearly seems to be an important factor in determining a material's creep resistance, but it is not the only term (there is still significant scatter in Figure R). Another factor which should be important is stacking fault energy. If stacking fault energy, γ, is high, dislocations will not dissociate and cross-slip will be relatively easy. Low stacking fault energy materials have widely separated partials, and cross slip is very difficult. Intuitively, this makes recovery processes more difficult. The effect normalized stacking fault energy on normalized strain (by modulus and diffusivity) is shown in Figure S.

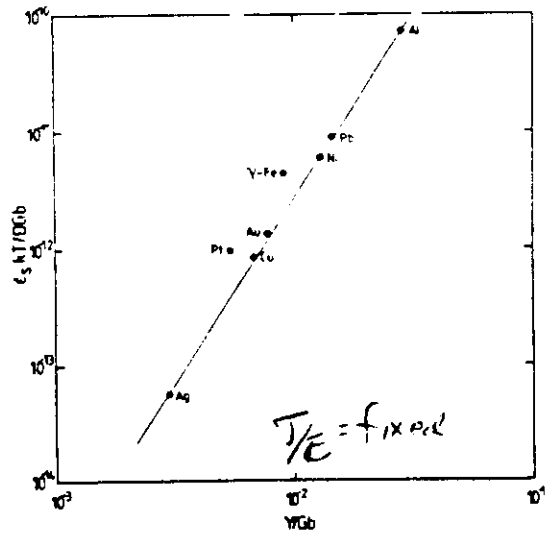

Figure S. Effect of normalized stacking fault energy on normalized creep rate. (Taken from Evans and Wilshire, data from Mukerjee et.al.[1])

Based on this we can improve our first-order equation to take on the form:

$$\dot{\varepsilon}_{ss} = AD_L \left(\frac{\gamma}{Gb}\right)^3 \left(\frac{\sigma}{E}\right)^5$$

---

1 A. K. Mukherjee, J. E. Bird and J. E. Dorn: *Trans. ASM*, 62, 155 (1969).

This has immediate utility in that we can use equations of this type to determine what materials and alloy additions are good candidates for creep performance. However, one element may not be satisfying. In diffusional creep we considered that more than one kind of diffusion path may be active (grain boundaries and the bulk). In real polycrystalline materials three kinds of paths are available: the bulk, grain boundaries and dislocation cores. Thus, the "effective diffusion coefficient"[1] should contain terms relating to each of these three paths:

$$D_{eff} = f_L D_L + A\rho D_p + B\frac{1}{d} D_{gb}$$

In this expression A and B are terms which relate to the effective widths of dislocation cores and grain boundaries, respectively. For the case of pipe and bulk diffusion, empirically it has been determined that:

$$D_{eff} = 100\left(\frac{\sigma}{E}\right)^2 D_p + D_L$$

The stress squared term follows from the Taylor relationship between dislocation density and flow stress and is consistent with experimental observations. Using this approach Luthy *et al* were able to correlate the steady-state flow stress of pure polycrystalline aluminum over 21 orders of magnitude, Figure T.

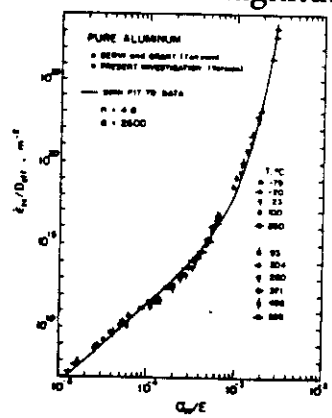

Figure T. Normalized stress v. strain rate for pure polycrystalline aluminum, using the effective diffusion coefficient concept (from Luthy, Miller and Sherby).

Following these concepts, at low temperatures, where pipe diffusion controls deformation, increasing stress increases the diffusion coefficient thus, we expect a strain rate sensitivity exponent of 7. This transition is observed at higher stresses and lower temperatures.

Further evidence for this concept comes from measured creep activation energies, Figure U. Typically the activation energy for pipe diffusion is about 0.6 of that for lattice self-diffusion.

---

[1] H. Luthy, A. K. Miller and O. D. Sherby: *Acta Metall*, 28, 169 (1980).

Now, if the subgrain size is fixed, either by a small grain size or dispersoids, it is expected that this equation will describe deformation. In such a case the flow stress, at fixed strain rate would take on a form similar to the Hall-Petch relationship. Specifically,

$$\sigma_{flow} = K\lambda^{\frac{-3}{8}}$$

The review by Nix and Gibeling[1] give a clear and fairly complete accounting of how changing structure, and the kinetics of structural change effect creep.

The other common interpretation of stress-change data[2] is that individual dislocations move under the influence of the applied stress, less an internal stress. If sufficiently large stress reductions are applied a stress change can be found at which there is a period at which there is a zero creep rate following the change. The low stress level is equated with an internal stress. Researchers with the former point of view argue that this part of the transient represents anelastic (time-dependent, reversible) deformation rather than plastic creep, and despite being structure-sensitive, is not directly relevant to the creep process.

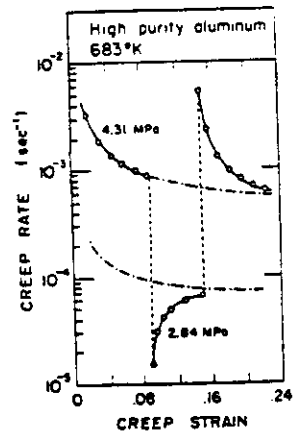

Figure W. Creep transients following stress changes in pure aluminum. (From Sherby, Klundt and Miller[3])

B) Theory

At the present time, there is no accepted comprehensive theory which treats all of the aspects of the creep of pure metals listed above. Weertman has noted[4] that all models of creep based on edge dislocation climb yield models with a stress exponent of three, provided that no un-natural assumptions are made. None of the current theoretical models for creep with exponents above three are fully satisfactory. The origin of the natural law is presented at the end of the next section.

---

1 *Flow and Fracture at Elevated Temperature*, proceedings (see first ref. list)

2 See Evans and Wilshire's book for a survey.

3 *Metall. Trans.*, 8A, 843, (1977).

4 J. Weertman in *Rate Processes in Plastic Deformation of Materials*, ASM, p. 315, (1975).

Class I Solid Solutions

A) Experimental Observations

Sherby and Burke noted that solid-solution metallic alloys could often be divided into two broad categories based on their behavior as follows:

Class I alloys	Class II alloys (pure metal-like behavior)
power-law stress dependence, n≈3	power-law stress dependance n≈5
no (or inverse) primary creep	large primary creep
SFE, γ, does not matter	SFE is important
Subgrains seldom form/not important	Subgrians form and are important.
faster than expected creep after stress drop	slower than expected creep after a stress drop
Interpretation:	
Dislocation glide controlled	Dislocation climb controlled

Class II behavior is the "pure metal" behavior, discussed previously. The following figures illustrate the kinds of behavior seen in Class I alloys.

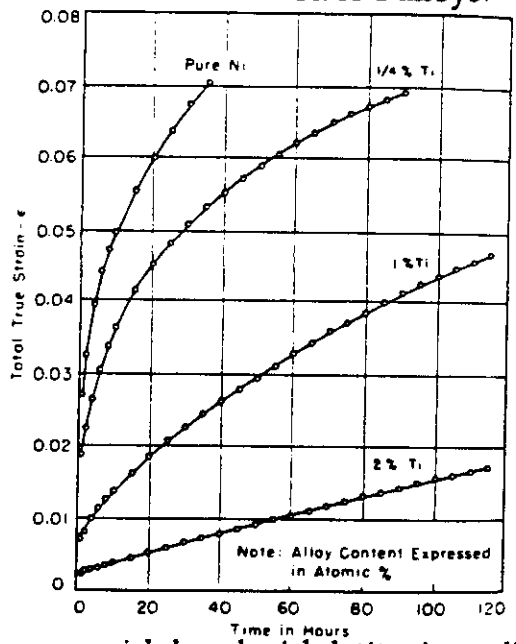

Figure X. Creep curves for pure nickel and nickel titanium alloys tested at 700°C and a stress of 5750 psi.[1]

[1] *Trans ASM*, **46**, 701 (1954).

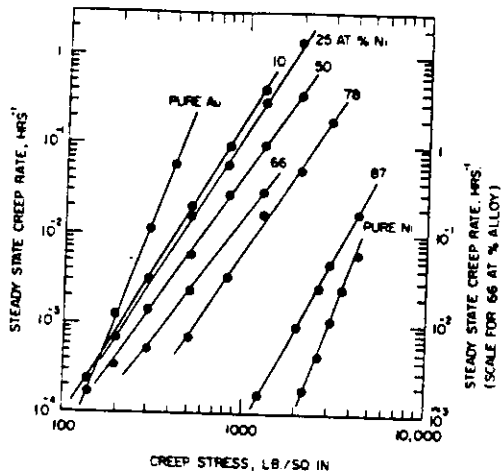

Figure Y. Steady-state creep-rate v. stress for a number of Au-Ni alloys at 960° C. Note that the pure metals have n≈5 and solid solutions have n≈3. (from Sherby and Burke).

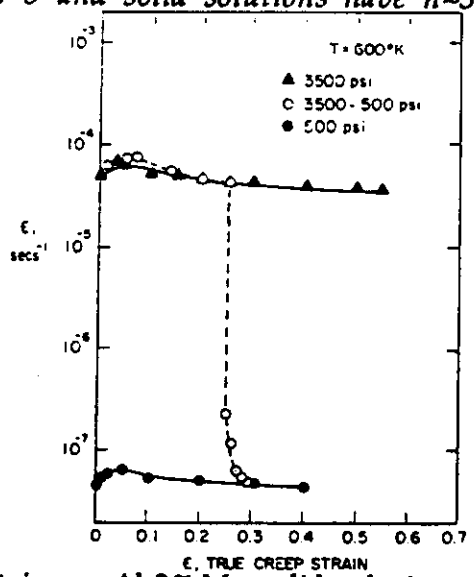

Figure Z. Stress change test in an Al-2%Mg solid solution at 600K. Note the difference in behavior compared to the pure Al. (from Sherby and Burke)

Not all solid-solution alloy systems show Class I behavior. Cannon and Sherby[1] have empirically noted that Class I systems tend to have large size differences between slovent and solute and the solvents tend to have low elastic moduli. This classification system is shown in Figure Aa.

[1] W. R. Cannon and O.D. Sherby: *Metall Trans*, **1**, 1030 (1970).

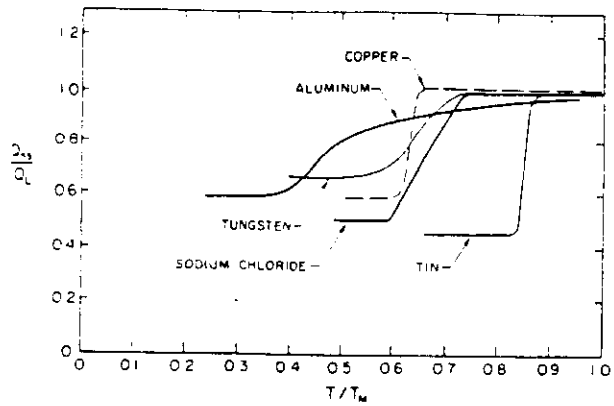

Figure U. Activation energies for steady state flow for a number of materials (from Luthy, Miller and Sherby)

Up to this point we have only considered the mechanical response of the material. Structural changes are also an important part of the creep process. In steady-state creep, the subgrain size is a function of the applied stress, and essentially independent of strain. Experimental data (Figure V) shows that the subgrain size is approximately inversely proportional to the applied stress for a large number of materials.

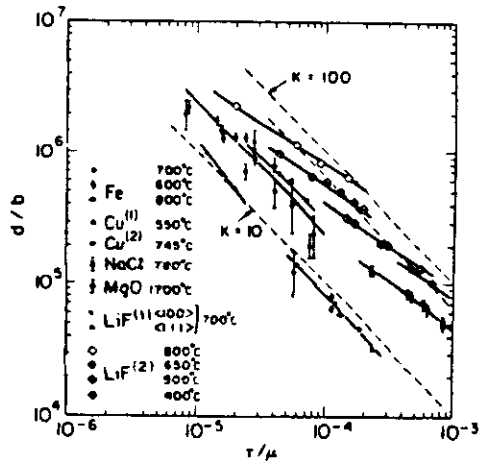

Figure V. Measured subgrain size as a function of the steady state flow stress for a number of materials (From Porier).

So far in this treatment, the mechanical response of the materials to a constant stress has been considered. Immediately after a stress change, pure metals show a larger change in stress that would be expected based on the usual stress exponent of 5. There are two (or more) ways to interpret this. One school of thought (see Sherby, Kludnt and Miller) argues that on a stress change, the subgrain size is fixed, and a new constitutive equation should be developed for constant structure conditions. Based on analyses of the kind shown in Figures V and W, they propose that the equation should take the form of:

$$\dot{\epsilon} = 2X10^{9}\frac{D_{eff}}{b^{2}}\left(\frac{\lambda}{b}\right)^{3}\left(\frac{\sigma}{E}\right)^{8}$$

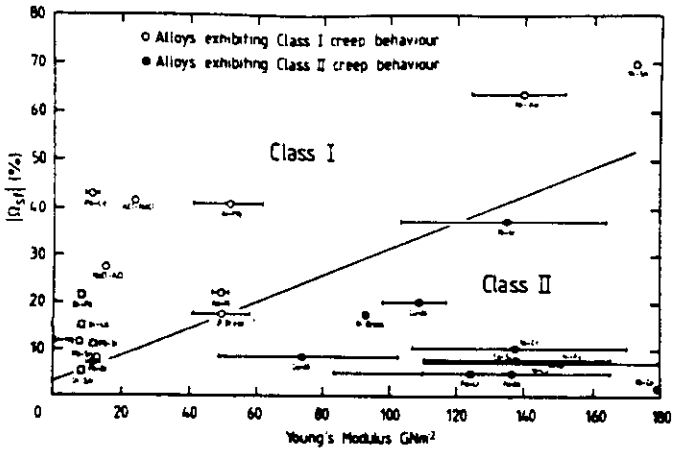

Figure Aa. size difference and elastic moduli (for the pure slovent) for a number of solid-solution alloy systems. The brackets give the range of modulus over the testing temperatures. (From Cannon and Sherby.)

It should be noted that while this classification scheme has great a great deal of experimental support and is of great practical use, there is often not a black-and-white classification for some alloys. Poirier's text points out some of the limitations of this classification scheme.

B) Theory

Again, plastic deformation is produced by the motion of discrete dislocations. In order for steady-state flow to take place dislocations must move long distances. However barriers are in place. Thus, both glide is required, and climb (or cross-slip, etc.) must act for dislocations to surmount barriers, as illustrated in Figure Ab.

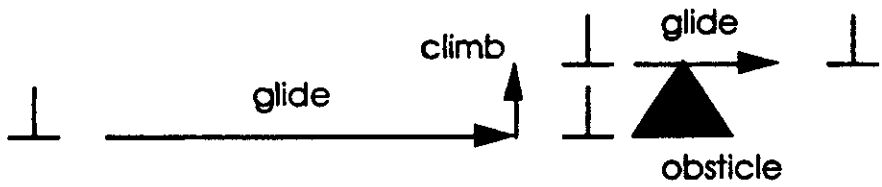

Figure Ab. Schematic diagram of a dislocation gliding to an obstacle.

In the case where solutes exist they may diffuse to the dislocation core. In this case, the motion of the solute atmosphere surrounding the dislocation core may be the rate limiting step. This situation was first analyzed by Weertman[1]. The key points are as follows.

$$\dot{\epsilon} = \rho v b$$

$$\rho = C\left(\frac{\sigma}{E}\right)^2$$

$$v = \sigma D_{solute}$$

[1] J. Weertman: *Trans AIME*, **218**, 207 (1960).

Therefore, $\dot{\varepsilon} = CD_{solute}\left(\frac{\sigma^3}{E^4}\right)$

The key to this is that climb and glide are sequential processes and therefore, the slower process will control the deformation rate. The resulting schematic stress v. strain-rate curve is shown in Figure Ac.

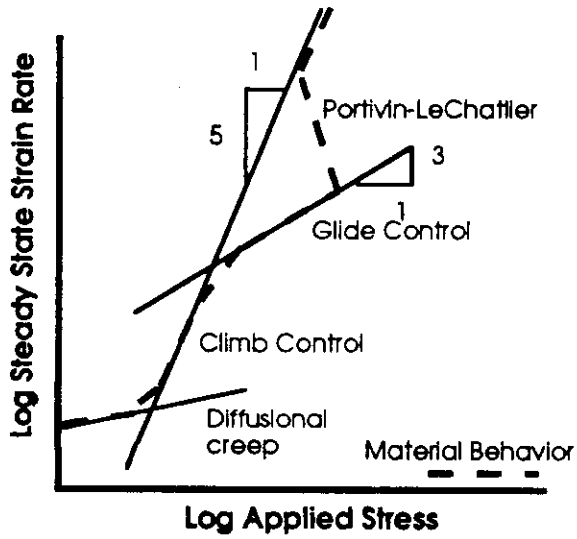

Figure Ac. Schematic creep curve of a Class I system. Diffusional, climb controlled, glide controlled and Portivin-LeChatlier creep are all shown. Note that both independent and sequential processes are represented.

One final point on the creep of solid solutions. The above graph suggests that the addition of solute will increase the strength of a solid. The previous example of carbon in austenitic steel shows this is not always the case.

Grain Boundary Sliding

Most of the discussion of grain boundary sliding will be deferred until the section on superplasticity. However, a few words are appropriate now. By experimental observation, grain boundary sliding is a mechanism distinct from slip creep and diffusional flow. For fine grained materials at intermediate temperature, creep may occur 200 or more times faster than predicted by coble creep, and strain discontinuities are noted at grain boundaries. Grain boundary sliding must be accommodated by either diffusional flow or slip in the grains. How accommodation occurs at these rates is still not fully understood.

Dispersion strengthened materials

When fine dispersions of very small particles (approx. 0.1μm inter-particle spacing) are added to a metal matrix, the creep behavior of the structure changes significantly. Specifically at low stresses the stress exponent increases significantly (threshold behavior) the activation energy for creep increases, and the overall strength of the material increases significantly. This will not be treated in detail here, but many factors are critically important including the particle size, inerparticle spacing, modulus

mismatch between particles and matrix and the interface condition between particles and matrix. Theoretically, there is currently debate whether dislocations are impeded by passing by particles (bowing, or climb) or by an attractive interaction between the particles and the dislocations, after they have passed[1].

The Big Picture -- Deformation Mechanism Maps and Phenomenological Equations

There are two basic approaches to understanding creep over wide ranges of stress, structure, temperature, and even material. One is by use of the Dorn (or Dorn-type) equations. The Dorn equation is stated:

$$\dot{\varepsilon} = AD_L \frac{\mu b}{kT}\left(\frac{\sigma}{\mu}\right)^n$$

Originally this was intended to describe slip-creep, but the efforts of Sherby and others have extended this equation by determining activation energies and stress exponents for a number of other mechanisms. Using this approach one can typically estimate the creep rates in an unknown system (above 0.6 T_m) within a factor of 100. This correlates to a prediction of flow stress within a factor of about two and one-half. The dependences for Qc, n and structure for other processes is shown below:

A Short Catalog of Creep Mechanisms

Mechanism	Temp. Dependence*	Stress Dependence	Structure Dependence	Conditions Where Observed
Diffusional				
Nabarro-Herring	D_l	$(\sigma/E)^1$	d^{-2}	Fine grains, low stress, hi T
Coble Creep	D_{gb}	$(\sigma/E)^1$	d^{-3}	Fine grains. low stress, hi T
Slip				
Viscous Glide (Class I Solid Sol.)	D_l	$(\sigma/E)^3$	$e^{-2}\, c^{-1}$	Misfitting solutes -- Glide controls creep. Climb and glide are sequential
Weertman's Climb Model	D_l	$(\sigma/E)^{4.5}$	$M^{-0.5}$	Pure Metals
Lattice Diff. Cont (Phenomenological)	D_l	$(\sigma/E)^5$	Stress fixes structure	Coarse grains, T>0.6Tm
Pipe diffusion control (Phenomenological)	D_p	$(\sigma/E)^7$	"	As above T= 0.4 to 0.6 Tm
Constant Structure D_l (Phenomenological)	D_l	$(\sigma/E)^8$	λ^3	Constant Structure Tests and ODS alloys T>0.6 Tm
Constant Structure D_p (Phenomenological)	D_p	$(\sigma/E)^{10}$	λ^3	As above, lower Temp range

[1] See For example, D. J. Strolovitz, *et al.*: *Acta Metall*, 31, p. 2151 (1983)
E. Artz and Rosler, *Acta Metallurgica*, 36, pp. 1043 to 1051 and 1053 to 1060.

Grain Boundary Sliding (Phemomenological)				
Lattice Diff. Cont.	D_l	$(\sigma/E)^2$	d^{-2}	Fine grains, intermed. T and σ
Pipe Diff. Cont.	D_p	$(\sigma/E)^4$	d^{-2}	As above, but lower T.
G. B. Diff. Cont.	D_{gb}	$(\sigma/E)^2$	d^{-3}	As above, maybe finer G.S.
Others				
Harper-Dorn Creep	D_l	$(\sigma/E)^1$ one Power	-	High T, Low σ, Coarse Grains

Terms

Subscripts
l- Lattice Diffusion
p- Diffusion along dislocation pipes
gb- Grain Boundary Diffusion

The General Forms:

$$\dot{\varepsilon}_{ss} = A\, D_{eff}\, S \left(\frac{\sigma}{E}\right)^n$$

$$D_{eff} = D_l + B\, D_{gb} + C\, D_p$$

$$D_x = D_x^0 \exp\left(\frac{-Q_x}{RT}\right)$$

Symbols
E- Dynamic Elastic Modulus
L- Linear Intercept G. S. (or interparticle size)
d- Grain Diameter =1.76 L
λ- L. I. Subgrain size
e- Fractional size diff. between solvent & solute atoms
c- Concentration of solute atoms
S- Generalized Structure Function
n- Stress exponent (n=(1/m); m-strain rate sensitivity exp)
M- Dislocation Source Density

The other common way to express behavior over wide ranges of stress and temperature is by deformation mechanism maps, which have been popularized by Frost and Ashby[1]. These are usually developed from both experimental data and analytical relations. An example from that book for polycrystalline nickel is shown below:

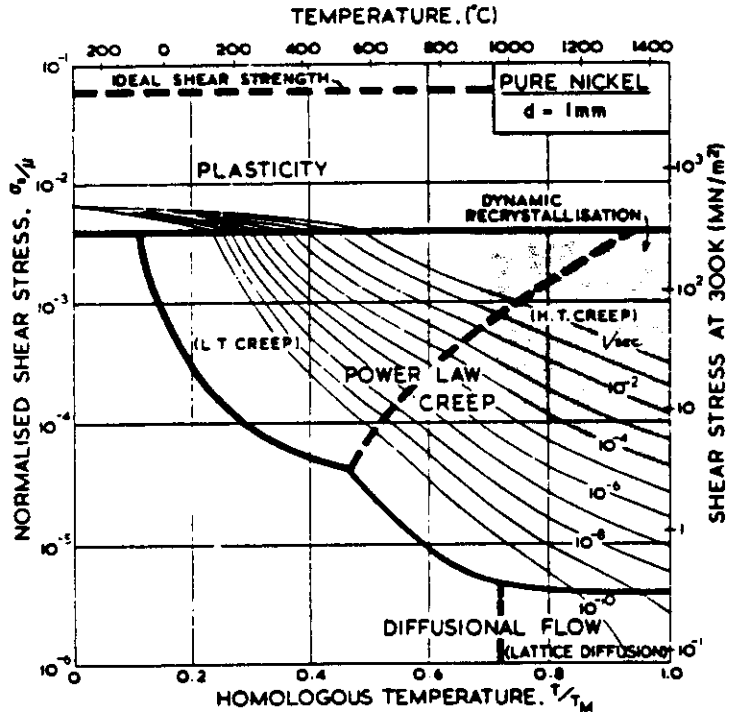

[1] H. J. Frost and M. F. Ashby: *Deformation Mechanism Maps*, Pergamon Press (1982).

C. Creep in Specific Systems

Comparison between metallic and ceramic creep

Differences

- Several sublattices (fully or partially occupied) exist. Ions of various charge and size exist on each sublattice.
- Complex point defect chemistry
  - Charge neutrality
  - Intrinsic vacancies from thermal activation
  - Extrinsic vacancies from impurities
  - For oxides stoichometry is a function of oxygen partial pressure
- Dislocations
  - Large Burgers' vectors
  - Kinks and jogs can be electrically charged

Similarities

Despite the differences listed above the situation is not very different than for metals (and more data and models exist for metals). Specifically:

- Diffusion still controls rates at elevated temperatures
  - (slowest species down fastest path)
  - (impurity and O_2 pressure must be carefully considered)
- Stress dependence also varies between 1 and 8 typically
  - (values near 1 are common at low stress, 3 or 5 are common at higher stress)
- Substructure development is essentially the same.
  - subgrain size is found vary inversely with stress.
  - dislocation density varies as stress squared.

Superplasticity[**]

basic principles

The phenomenon which give superplasticity its name is the tremendous tensile elongations which are available from superplastic materials. This comes about from the high strain rate sensitivity exponent, m (m=1/n). To understand why a high stress

---

** Some Reviews of Note:

Padmanbahn and Davies: *Superplasticity*, Springer-Verlag, (1980).

O. D. Sherby and J. Wadsworth: "Development and Characterization of Fine-Grain Superplastic Materials", *Deformation Processing and Structure*, G. Krauss, ed., ASM (1984).

B. P. Kashyap, A. Arieli and A. K. Mukherjee: "Review Microstructural Aspects of Superplasticity", *J. Mat. Sci.*, **20**, p. 2661 (1985).

J. Edington, K Melton and C. Cutler, "Superplasticity", *Progress in Materials Science*, **21**, 1 (1976).

R. H. Johnson: "Superplasticity", *Metall Rev.* Review no. 146, pp. 115-134 (1970).

T. G. Langdon: "The Mechanical Properties of Superplastic Materials", *Metall Trans*, **13A**, p. 689 (1982).

exponent enhances ductility consider a tensile bar with a small area with a reduced cross section. Note that m can be defined as:

$$m = \left(\frac{\delta \log \sigma}{\delta \log \dot{\varepsilon}} \right)$$

If the imperfection is to grow, the strain rate there must exceed that in the rest of the sample. If m is high, there will be a large increase in the local flow stress, resisting the deformation. Woodford[1] showed that for a large number of materials tensile elongation correlates well with m-value as is shown below:

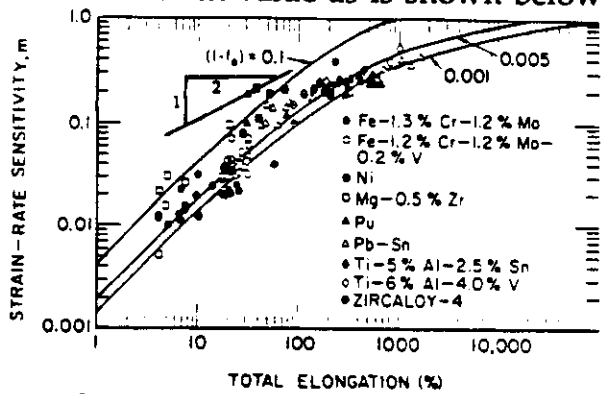

The minimum structural prerequisites for superplasticity are:

1) Small and stable grain size (<10μm)
   a second phase is often needed to stabilize this small grain size
2) Boundaries can support a tensile stress and retain mobility
3) High angle boundaries are present
4) Strengths of different phases must be comparable (or cavitation)

The usual experimental observations are:

Either

There is a constant m of approximately 0.5 until slip creep is active

or

m varies, reaching a maximum (up to 0.9) at intermediate rates

- There is discrete motion across grain boundaries
- Grain growth is enhanced by deformation
- Grains rotate
- Grains remain equiaxed
- Any initial texture is usually destroyed

Also, General form of Eqn

$$\dot{\varepsilon} = A D_{eff} \left(\frac{\sigma}{E}\right)^n \left(\frac{b}{d}\right)^p$$

$n \sim 1-3 \qquad p \sim 2-3$

Mechanistically explanations center on the accommodation of grain boundary sliding by:

- Deformation by lattice diffusion
- Deformation by grain boundary diffusion
- Different behavior of the near-boundary region
- GBS accommodation by slip

---

[1] W. B. Morrison: *Trans Met Soc AIME*, **242**, 2221 (1968).

- GB migration taking an important role in accommodation.

Superplasticity in Zirconia

Recently, Wakai[1] *et al* have shown that a completely crystalline ceramic can be made superplastic in tension. This is shown graphically below:

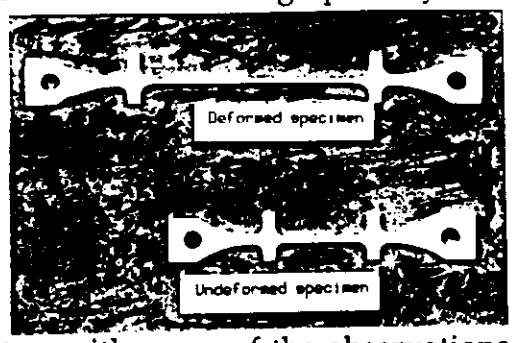

It is significant to note that as with many of the observations of superplasticity in metals, this material exhibited a stress exponent of approximately 2. A recent TEM study has also shown that the grains remain fairly equiaxed up to 100% strain[2]. Although grain growth still does occur in this system

Very recently attention has shifted to composites of zirconia and alumina[3] with this two phase system, finer grain sizes should be stabilized, and grain growth should be inhibited. These approaches hold great promise for new routes for high quality near-net shape forming of ceramic materials.

D. High Temperature Cavitation and Crack Growth**

In Summary: at elevated temperatures, it is the same fundamental processes which drive both plastic deformation and fracture.

Types and Mechanisms of Damage

The below figure, taken from Ashby *et. al.* [4] schematically illustrates the kinds of damage which accumulate and lead to fracture at elevated temperature.

---

1 F. Wakai, S. Sakuchi and Y. Matsuno: *Adv Ceram Mat*, **1**, 259 (1986).

2 R. Duclos, J. Crampton and B. Amana: *Acta Met.*, **37**, 877 (1989).

3 H. Wakai and H. Kato: *Adv Ceram Mat*, **3**, 71 (1988) and T. G. Nieh, C. M. McNally and J. Wadsworth: *Scripta Met.*, **23**, 457 (1989).

** Outstanding overviews of elevated temperature fracture are available from Nix and Gibeling (in *Flow and Fracture at Elevated Tempeatures*, R. Raj, ed., ASM 1985.) and *Perspectives in Creep Fracture*, M. F. Ashby, ed., Permagon Press, 1983. This section is based largely on these presentations.

4. M. F. Ashby, C. Ghandi and D. M. R. Taplin: *Acta Met.*, **27**, 699 (1979).

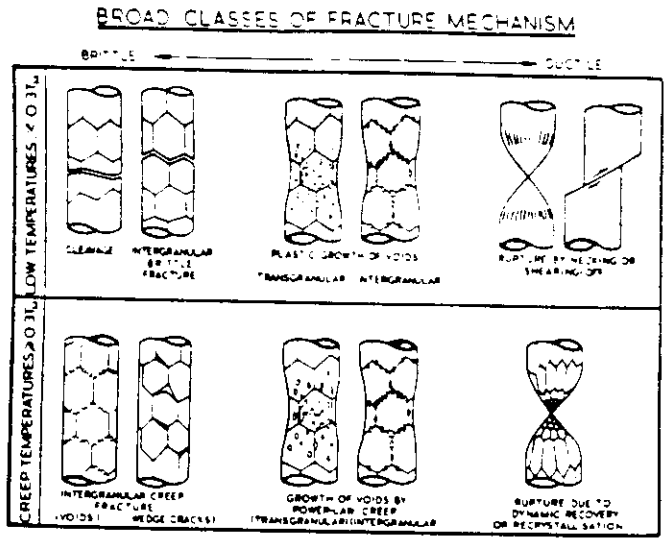

The prominent difference between low and high temperature fracture is that self-diffusion 1) limits work-hardening in the material, yielding power-law creep and 2) diffusive flow of material is now possible. Thus, at elevated temperatures fracture is dominated by the growth and linkage of cavities at grain boundaries or second phase particles.

Nucleation of voids

It can be shown that the stresses required for the thermal activation of supercritical vacancies are too high to explain the early nucleation of grain boundary voids observed in metals and ceramics. The figure below taken form Nix and Gibeling show how a number of microstructural features can lead to nucleation of voids at grain boundaries. It is important to note that even in very pure metals, steps at grain boundaries or slip bands can nucleate a void.

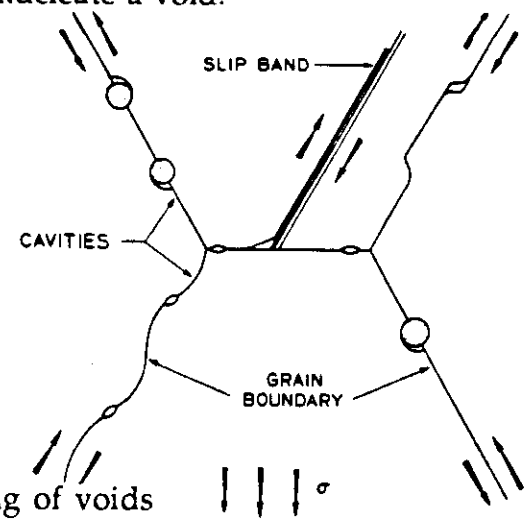

Growth and interlinking of voids

It can be inferred both from experimental observations and theoretical treatments that void growth is closely related to overall plastic deformation. First, Grant and Monkman have empirically shown that time to creep rupture and creep rate are inversely related. This can be simply stated as:

$$\dot{\varepsilon}_{ss} t_r = C_{G-M}$$

Here, t_r is the time to rupture and $C_{G\text{-}M}$ is the Grant-Monkman constant which is a material constant. This relationship simply implies that for one material, the amount of strain expected during steady state creep is a constant. Thus, the rate of plastic flow and void growth seem to be inter-related. The data of Dennison and Wilshire[1], on nickel with varying impurity content, replotted by Nix and Gibeling, is shown below. This shows that the Grant-Monkman relation is satisfied over a very wide range of strain rate and stress and temperature.

From a mechanistic point of view, voids can grow on grain boundaries by a combination of surface and grain boundary diffusion as was suggested by Hull and Rimmer[2]. This is illustrated below. If these cavities grow only on boundaries which oriented roughly perpendicular to the tensile axis, then the strain associated with the cavity growth will un-load that boundary, shedding load to other parts of the structure. If the structure does not creep, the driving force for cavity growth will cease. Thus plastic deformation is required for this constrained cavity growth process. This treatment was first suggested by Dyson[3] and a three-dimensional analysis of the stress-shedding was recently performed by Anderson and Rice[4].

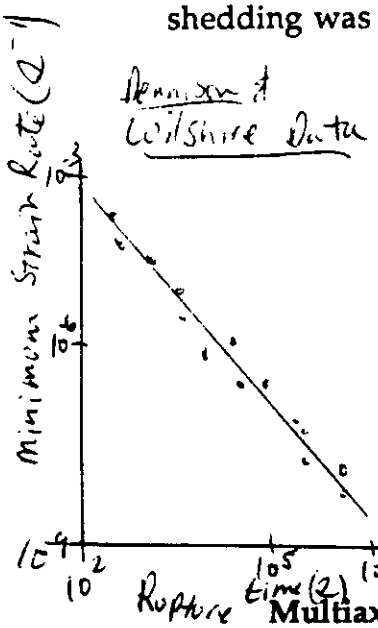

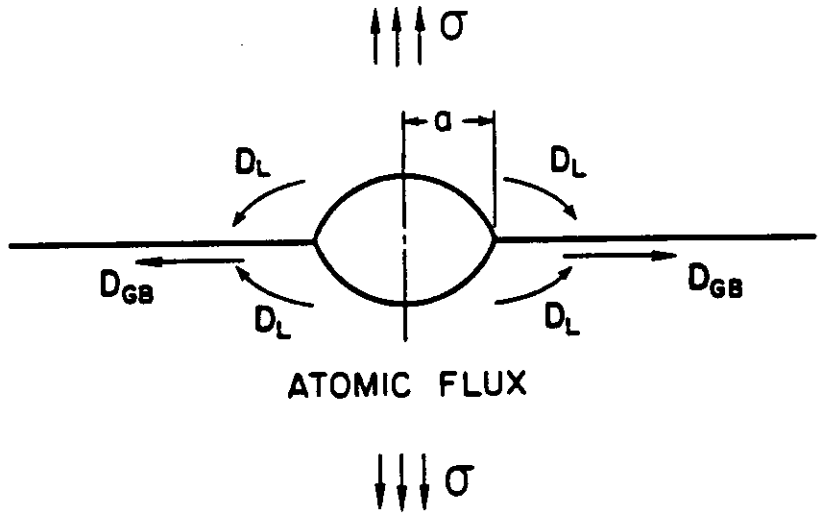

Multiaxial Stress States

One of the problems in creep rupture which has been troubling has been the prediction of rupture life under multiaxial states of stress. On a first order, one expects that as the principal tensile stress, and the hydrostatic part of the stress state increase, time to rupture will decrease, since void growth has a larger driving force. Quantitative predictions of fracture lives has proven difficult. Nix *et al* [5] have used parts of the analysis of Anderson and Rice to suggest that the "principal facet stress", the stress seen on grain boundaries oriented perpendicular to the tensile direction is a very good

---

1 J. P. Dennison and B. Wilshire: *J. Inst Metals*, **91**, 343 (1962).
2 D. Hull and R. E. Rimmer: *Phil Mag*, **4**, 573 (1959).
3 B. F. Dyson: *Metal Sci*, **10**, 349 (1976).
4 P. M. Anderson and J. R. Rice: *Acta Metall.*, **3**, 409 (1985).
5 W. D. Nix, J. C. Earthman, G. Eggeler and B. Ilshner: *Acta Metall*, **37**, 1067 (1989).

correlation parameter for creep under multiaxial loading. The value of the principal facet stress, σ_F can be expressed as:

$$\sigma_F = 2.24\sigma_1 - 0.62(\sigma_2 + \sigma_3)$$

The figures below show the successes of this life estimation parameter. The paper also discusses some situations in which this correlation approach fails.

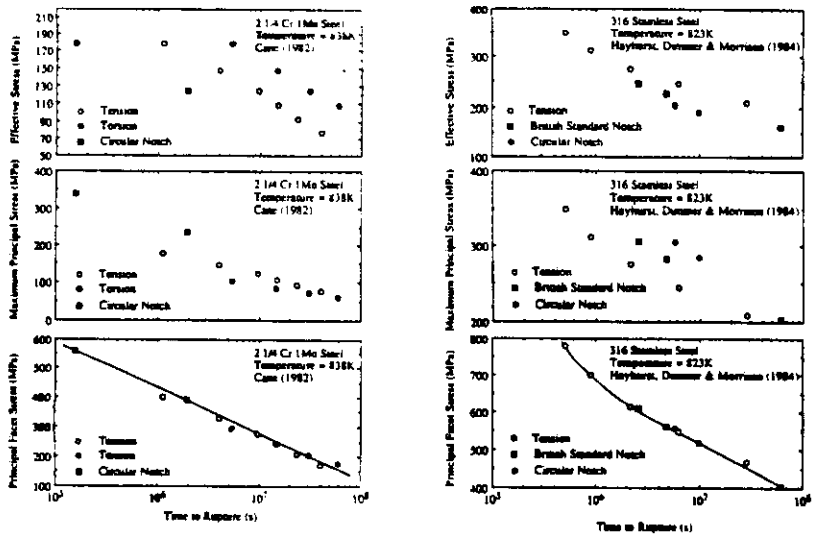

Crack Growth at elevated Temperature

Finally, it is important to note that the stress field in front of a crack in a creeping material is quite different than that in a linear elastic material[1]. In a linear elastic material the stress distribution at the front of a crack tip is characterized the stress intensity factor K_I as:

$$\sigma_{ij} = \frac{K_I}{\sqrt{2\pi r}} f_{ij}(\theta)$$

In a creeping material a different stress distribution (characterized by C*) is developed the form of the stress field is:

$$\sigma_{ij} = \left(\frac{C^*}{r}\right)^{\frac{1}{n+1}} g_{ij}(\theta)$$

where n is the stress exponent. Thus, the stress field in front of the crack tip is controlled by the creep processes in the material.

---

[1] H. Ridel and J. R. Rice: in *Fracture Mechanics: Twelfth Conference*, ASTM STP 700, Ed. E. C. Paris, ASTM, p. 112 (1980). and H. Ridel: *J. Mech Phys Solids*, 29, 35 (1981).

E. Effects of Internal Stresses

In Summary: Isothermal creep behavior is nearly irrelevant in understanding the actual (temperature changing) behavior of "composites". In this context, composites are aggregates of different or anisotropic materials. (internal strain mismatches develop).

Introduction

For a number of years it has been recognized that differences in the coefficients of thermal expansion in composite materials can have important and deleterious effects on their mechanical behavior. Many studies have shown that thermal cycling can induce plastic deformation of the matrix, dimensional instability[1], reinforcement damage[2,3], and interfacial damage[4,5]. Furthermore, fracture toughness and elastic modulus can be reduced[6], and creep accelerated[7-13]. With the current strong interest in identifying and developing high temperature composite materials, it is important that a fundamental and general understanding of these issues is developed, especially in regard to elevated temperature deformation. Furthermore, since most commercial high temperature alloys contain phases which have dissimilar coefficients of thermal expansion, an understanding on how thermally induced strains and stresses influence deformation may be useful for improving life prediction with these materials.

Background

EXPERIMENTAL OBSERVATIONS

It is appropriate to first give some examples of the kinds of phenomena which have been reported in the deformation of metal matrix composites under thermal cycling conditions. The elevated temperature deformation of aluminum-silicon carbide composites has been studied under isothermal[15] and thermal cycling[8,11,14-17] conditions by a number of researchers. A number of consistent observations can be found in these works. Figure 1 from Pickard and Derby[15] shows typical creep curves derived from an Al-SiC composite crept under isothermal and thermal cycling conditions. Examination of these curves reveals the following:

❄ Under thermal cycling conditions, primary creep is eliminated, and strain rate is not a strong function of strain or time.

❄ Tertiary creep can be greatly delayed. In the present example, the deformation rate begins to increase after 2-3 percent strain in the isothermal case, whereas under thermal cycling, stable steady-state creep is obtained at 16% tensile elongation.

Sherby *et. al.* [8,9,11] have measured and analyzed the steady state strain rate in Al-SiC whisker-reinforced composites as a function of stress under thermal

cycling conditions. Figure 2 is based on this work, carried out in compression[8]. This figure shows:

❄ Thermal cycling can weaken the composite dramatically, as compared to the isothermal behavior at the highest temperature of the cycle.

❄ At low applied stresses, under thermal cycling conditions, the composite shows a very high strain-rate-sensitivity exponent (usually m~1). This m-value is similar to those seen in superplastic materials, and viscous liquids (i.e. molten glass or molasses).

Since the material shows a high strain-rate-sensitivity exponent, necking is inhibited[19]. Also since deformation can occur at relatively low applied stresses, microvoid initiation and coalescence seem to be inhibited. Both of these factors lead to the extremely large tensile elongations which have been observed under low stress thermal cycling conditions [8,15-17]. Figure 3 shows a dramatic example of how superplasticity can be induced in an Al-SiC whisker-reinforced composite[20].

The kinds of effects listed above are not restricted to the thermal cycling of Al-SiC; the effect is somewhat more general. There are several conditions in which stresses, and plastic strain, may be developed in a material in the absence of applied load. Three examples of this are:

1) *Thermal cycling of aggregates of anisotropic crystals or dissimilar materials.* In the thermal cycling of Al-SiC composites, Al has a coefficient of thermal expansion approximately $20X10^{-6}$ C^{-1} greater than SiC. Therefore, if the temperature of a stress-free composite changes by more than about 50^{o} C, plastic deformation will be produced in the aluminum matrix. As another example, in zinc, the coefficient of thermal expansion in single crystals is more than twice as great along the *c* axes as along the *a* axes. Thus, when polycrystalline zinc is subjected to a temperature change, the differing local dimensional changes produce stresses at the grain boundaries. A sufficiently large temperature change will therefore induce plastic flow. If the temperature is cycled repeatedly, internal plastic deformation will continue.

2) *Phase transformations.* Upon a phase transformation, volume changes produce misfit strains at the boundaries between transformed and un-transformed components. If the volume change is large enough, plastic deformation will accompany each phase change.

3) *Radiation swelling.* Neutron irradiation also changes the shape of many individual crystals. For example, upon irradiation α-uranium single crystals swell along the *b* axis and contract along the *a* axis. Again, the misfit at grain boundaries in a polycrystalline specimen may induce plastic flow.

Several studies have been carried out on materials in the above conditions, often a small stress is imposed on the sample. Regardless of the way internal plastic deformation is induced, the material behavior in these conditions is very similar. Specifically, the following effects have been reported in several systems:

1) Materials are often dimensionally unstable. Large irreversible strains may occur in the absence of an applied load.[13,21,25]

2) Materials can flow at stresses far beneath their usual yield stress (even the yield stress at the highest temperature of the cycle).

3) The strain-rate-sensitivity exponent is very close to one in many circumstances.

4) Very high tensile ductility has been seen in a number of these systems. This can be attributed to the low stress exponent[19].

Physically, this enhanced deformation may be explained as follows. Upon heating, transformation, or swelling, dimensional mismatches develop at grain boundaries producing internal stress. If the stress becomes large enough, internal plastic yielding will occur. On the reverse cycle (cooling or reverse transformation) plastic deformation may again occur. However, there is no assurance that the shapes of the grains will return to those at the beginning of the cycle. For random polycrystals, the strains on the cooling usually reverse those from the heating. However, if an external stress is applied, it influences the local deformations such that there is a non-reversed strain component in the direction of the applied stress. Most of the work of deformation, however, is done by the expansion mismatch. The result of this sequence of events is that the material exhibits a very low macroscopic flow stress, and the plastic strain per cycle will be proportional to the applied stress (at low applied stresses). It is expected, therefore, that whenever a material has plastic deformation induced internally it may deform more easily than a material that does not.

Experimentally, these effects have been well documented in a large, but limited, number of systems. The vast majority of experiments involve deformation concurrent with thermally induced phase transformations. The deformation behavior of a small number systems which contain internal thermal expansion mismatches have been studied under thermal cycling (Al-SiC composites, polycrystalline zinc[9] and uranium[10]). These systems show dramatic increases in deformation rates at low stresses under thermal cycling conditions. Recently, Chen and Daehn[22] have demonstrated that the thermal cycling of an Al-Si eutectic alloy will produce the same features (drastically reduced flow stress, and enhanced ductility) under low stress creep. It is believed that these effects are also likely to be important in many material systems currently used at high or variable temperature, since most engineering materials typically contain at least two phases which have different coefficients of thermal expansion. But, there has been virtually no experimental

examination of common engineering materials under thermal cycling conditions.

GENERALIZED LEVY VONMISES RESULT

Several researchers[17,23,24] have pointed out that all of the above effects are consistent with a continuum model based on the Levy-vonMises flow law. For a plastically deforming body, this equation relates the deviatoric stress imposed on the body to the plastic strain increment as:

A simple example of an application of the Levy-vonMises flow law to a composite deformation under changing temperature is given in Figure 4. For a hypothetical composite with long fibers, one can assume that: 1) the matrix has a much larger coefficient of thermal expansion than the matrix, and the temperature is cycled over a large enough range to induce plastic deformation of the matrix, 2) there is perfect bonding at the fiber/matrix interface, 3) The fibers are purely elastic and the matrix is elastic-plastic vonMises material with a temperature independent flow stress σ_0, 4) A shear stress is externally imposed on the composite and 5) temperature change induces a pure axial stress. Under these assumptions, the stress state which arieses in the matrix is shown in the right drawing of Figure 4. When the matrix is deforming plastically, this stress state can be represented as:

$$\sigma_{ij} = \begin{bmatrix} 0 & \tau_{xy} & 0 \\ \tau_{xy} & \sigma_y & 0 \\ 0 & 0 & 0 \end{bmatrix} \quad \text{on cooling} \qquad \begin{bmatrix} 0 & \tau_{xy} & 0 \\ \tau_{xy} & -\sigma_y & 0 \\ 0 & 0 & 0 \end{bmatrix} \quad \text{on heating}$$

Upon subtracting the hydrostatic component from these stress states, the deviatoric stress state can be represented as:

$$\sigma'_{ij} = \begin{bmatrix} \frac{-\sigma_y}{3} & \tau_{xy} & 0 \\ \tau_{xy} & \frac{+2\sigma_y}{3} & 0 \\ 0 & 0 & \frac{-\sigma_y}{3} \end{bmatrix} \quad \text{on cooling} \qquad \begin{bmatrix} \frac{+\sigma_y}{3} & \tau_{xy} & 0 \\ \tau_{xy} & \frac{-2\sigma_y}{3} & 0 \\ 0 & 0 & \frac{+\sigma_y}{3} \end{bmatrix} \quad \text{on heating}$$

Upon a complete thermal cycle, the diagonal terms cancel. Furthermore, since the fibers and matrix are bonded, their lengths cannot change independently. Therefore, the matrix axial strain must be fully reversed on heating and cooling. Thus, the only un-reversed plastic strain will be the shearing between fibers. Based on these equations, the shear strain per cycle can be calculated as:

$$\gamma_{xy} = 6\left(\frac{\Delta\alpha(\Delta T - \Delta T_{crit})}{\sqrt{\sigma_0^2 - 3\tau_{xy}^2}}\right)\tau_{xy}$$

ΔT_{crit} is the critical temperature change required to induce plastic deformation of the matrix. If the applied shear stress is much less than the matrix yield stress, this expression will reduce to :

$$\gamma_{xy} = 6\Delta\alpha(\Delta T - \Delta T_{crit})\left(\frac{\tau_{xy}}{\sigma_o}\right)$$

This simple analysis shows that thermal cycling of a composite with an elastic-plastic matrix can induce shear strains even if the applied shear stress is far less than the yield stress of the matrix, and that for small applied shear stresses, the shear strain per cycle will be proportional to the applied stress.

This analysis can be easily extended to other simple geometries, and the basic conclusion is always the same: If thermal cycling plastically deforms the matrix, the material will irreversibly strain under small loads and the strain per cycle (or strain rate under cycling conditions) will be proportional to the applied stress. If numerical methods are employed, one can also easily incorporate realistic material constitutive laws.

It should also be noted that very similar weakening and high strain-rate-sensitivity behavior have been predicted for systems in which both components of a fiber reinforced composite deform under thermal cycling[13]. The analysis of these systems is somewhat more complex since the volume fractions and constitutive behavior of both components have important effects on the composite's macroscopic behavior.

Recently, Daehn and Gonzalez-Doncel have proposed a model based on a stress and stain analysis which is equivalent to the Levy-vonMises rule, a matrix material which obeys thermally activated power law creep, and a time-stepping numerical solution[17]. They have shown that this first-order model yields predictions which are consistent with experimental observations of the thermal cycling of Al-SiC whisker reinforced composites. Figures 5 and 6 show comparisons between the predictions form the model and experimental data. Figure 5 shows the variation in steady-state strain rate as a function of applied stress, for a fixed thermal cycling condition. Figure 6 shows the variation in the steady-state strain rate as a function of the thermal cycle amplitude, with fixed applied stress. It is important to note that the model contains no curve fitting factors. All of the input data is obtained from the literature or from the results of experiments run under isothermal conditions. ~~These predictions are presented in detail in the paper, which is presented in Appendix III~~.

ASSUMPTIONS AND CAVEATS

While the Daehn/Gonzalez-Doncel model is believed to contain the physical essence of the composite thermal cycling problem, and has been shown to be consistent with a the observed thermal cycling behavior of Al-SiC, this model is based on a number of assumptions which may not be strictly valid.

Most importantly, in order to make the model simple and intuitive a very simple matrix stress state was assumed. It is not known to what extent these simplifications affect the results predicted by the model. Further experiments and modeling can shed light on this issue.

Figures Relating to the Effects of Internal Stresses

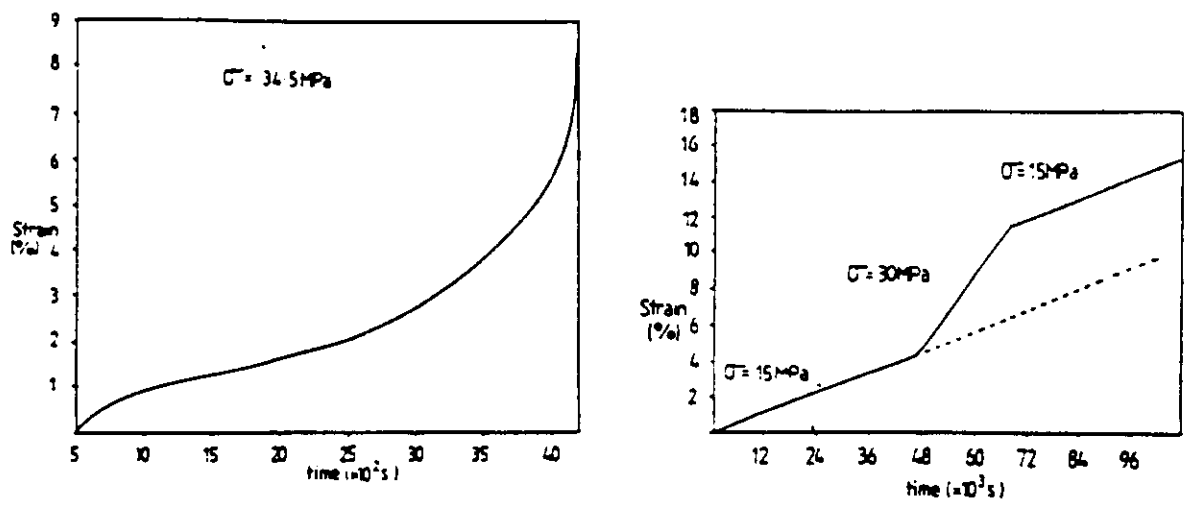

Figure 1. Creep curves obtained from an 1100 aluminum reinforced with 20 volume percent SiC particles. The right curve was obtained with isothermal testing at 350°C at an applied stress of 34.5 MPa. The curve on the left was obtained at with thermal cycling between 150° C and 350° C with a 420 s cycle period. Note that thermal cycling eliminates primary creep, increases the creep rate, and enhances ductility. (after Pickard and Derby, ref. 15.)

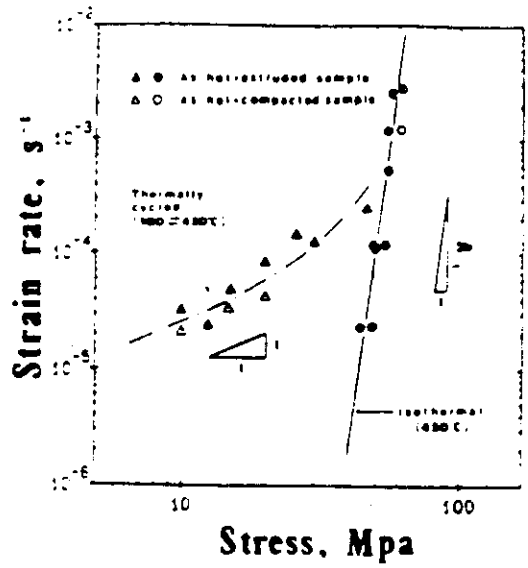

Figure 2. Influence of stress on the steady state creep rate of 20% SiC whisker reinforced 2024 alumium alloy tested in compression. (from Wu and Sherby[8]) Note that at low applied stresses, thermal cycling induces a strain-rate-sensitivity-exponent of one and the strain rate is greatly increased relative to isothermal behavior at the same stress. At high applied stresses the internally generated stresses have relatively little effect.

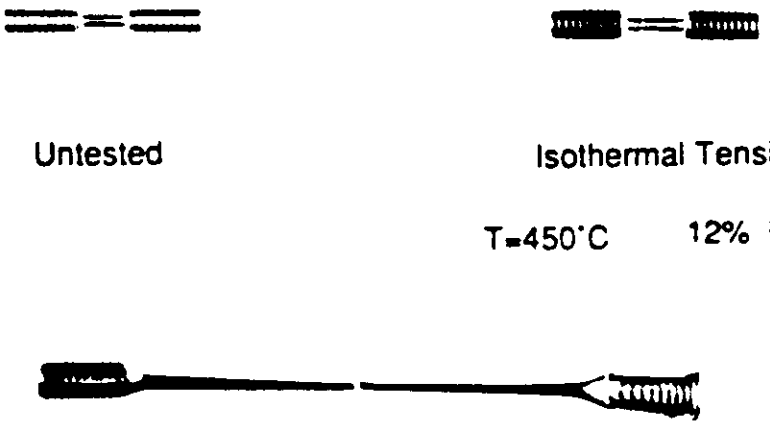

Figure 3. This photo illustrates the enhancement of ductility which is possible by thermally cycling a 6061 aluminum-20 volume percent SiC whisker-reinforced composite. The upper left sample was deformed at a low strain rate (~10^{-3} s-1) at 450° C, and shows approximately 12% tensile elongation at failure. The lower sample was thermal cycled (100° C-450° C, 200 s period) for several hours with a small applied stress (about 10MPa) and shows in excess of 1000% tensile ductility. (Photo courtesy of G. Gonzlez-Doncel)

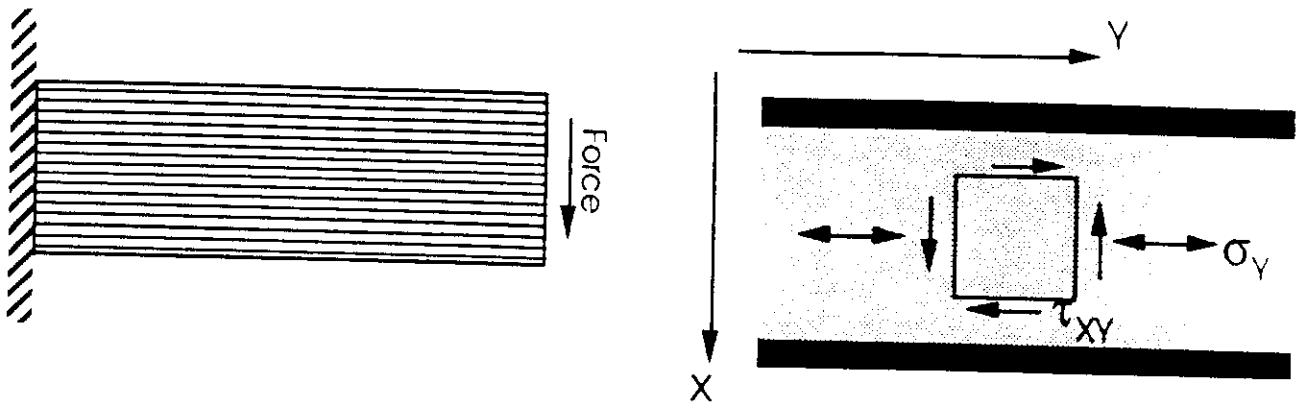

Figure 4. Schematic diagram of a whisker reinforced composite subjected to a shear stress and temperature change. The right part of the figure shows stress state in the matrix. The axial stress which is developed by the temperature change and the shear component results from the applied forces.

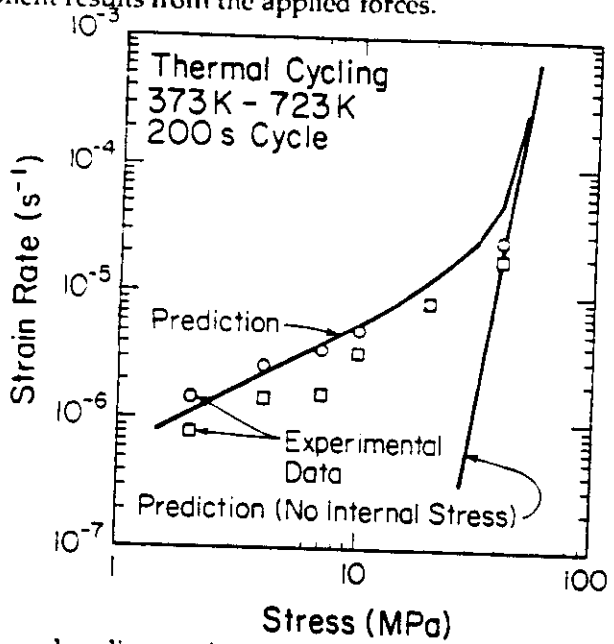

Figure 5. Thermal cycling strain-rate as a function of applied stress. The solid lines show the behavior under thermal cycling which is predicted by the model of Daehn and Gonzalez-Doncel, with and without a thermal expansion mismatch. The points represent experimental behavior, from two series of experiments. Both the simulations and experiments were run using Al-SiC (20 volume percent whskers) under thermal cycling conditions of 373 K to 723 K, in 200 second cycles.

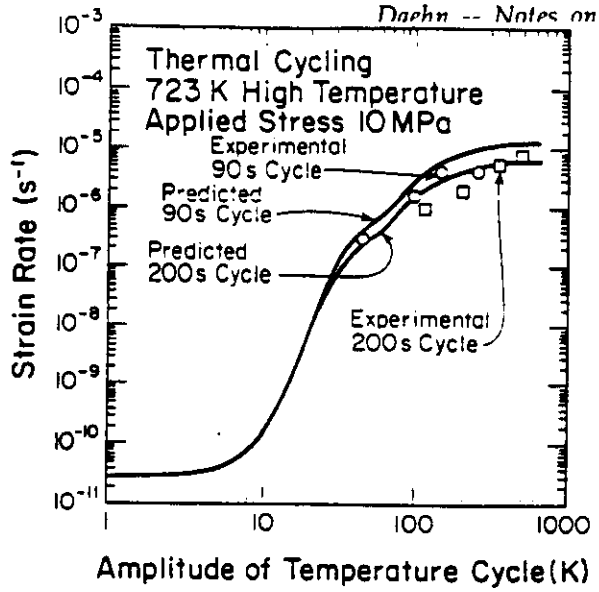

Figure 6. Comparison of the data of the Daehn/Gonzalez-Doncel model. In both the prediction and the experiments, the applied stress was 10 MPa and thermal cycles with a high temperature of 723 K, and an variable amplitude were imposed. Two thermal cycling periods (90 seconds and 200 seconds) were used. Again, there is good agreement between the preciction and experimental data, both in terms of trend and magnitude.

References Relating to the Effects of Internal Stresses

1. C. W. Marschall and R. E. Maringer: *Dimensional Instability an Introduction*, Permagon Press, Oxford, 1977, pp. 139-212.
2. G. Garmong and C.G. Rhodes: *Proc. of Conf. on In-Situ Composites, vol. I*, p251, National Acadamey of Sciences, 1973.
3. G. Garmong: *Metall. Trans.*, 1974, vol. 5, pp. 2199-2205.
4. S. Yoda, N. Kurihara, K. Wakashima, and S. Umekawa: , *Metall. Trans*, **9A**, pp. 1229-1236 (1978).
5. W. G. Patterson and M Taya: "*Proc. ICCMV*, Ed. W. C. Harrigan, J. Strife and A. Dhingra pp. 53-66 (1985).
6. W. S. Johnson: *ASTM Proc on Thermal Mechanical Behavior of Metal and Ceramic Matrix Composites*, Atlanta, 1988.
7. E. Gautier, A. Simon, and G. Beck: *Acta Metall.*, 1987, vol. 35, pp. 1367-1375.
8. M. Y. Wu and O. D. Sherby: *Scripta Met.*, 1984, vol. 18, pp. 773-776.
9. M. Y. Wu, J. Wadsworth, and O. D. Sherby: *Metall. Trans*, 1987, vol. 18A, pp. 451-462.
10. R. C. Lobb, E. C. Sykes and R. H. Johnson: *Metal Sci.J.*, 1972, vol. 6, pp. 33-39
11. G. S. Daehn and T. Oyama: "The Mechanism of Thermal Cycling Enhanced Deformation in Whisker-Reinforced Composites", *Scripta Metall,*. **22**, pp. 1097-1102 (1988).
11. S. H. Hong, O. D. Sherby, A. P. Divecha, S. D. Karmarkar, and B. A. MacDonald: *J. Compos. Mater.*, 1988, vol 22. pp. 102-123.
13. G. S. Daehn: , *Scripta. Metall,* (~~in press~~) **23**, (2), 1989. (Pg. 247)
14. J. C. Le Flour and R. Locicero: *Scripta Metall.*, 1987, vol. 21, pp. 1071-76.
15. S. M. Pickard and B. Derby: *Proc. 9th RISO Int. Symp on Met and Mat. Sci*, Ed. S. I. Anderson, pp. 447-452 (1988).

16. G. Gonzalez-Doncel, S. D. Karmakar, A. P. Divecha and O. D. Sherby: *Comp. Sci. and Tech.* , in press, (1989).
17. G. S. Daehn and G. Gonzalez-Doncel: ~~Submitted to *Metallurgical Transactions*~~, October 1988. (In Press)
18. T. G. Nieh: *Metall Trans.*, 1984, vol.15A, pp. 139-146.
19. E. W. Hart: *Acta Metall.*, **15**, pp. 351-355 (1967).
20. G. Gonzalez-Doncel: Unpublished research, Stanford Univeristy, 1987.
20. J. E. Burke and A. M. Turkalo: *Journal of Metals*, 1952, vol 4, pp. 651-656.
22. K. Wakashima, T. Kawakubo and S. Umekawa: , *Metall. Trans.*, **6A**, pp. 1755-1760 (1975).
22. Y. C. Chen and G. S. Daehn: Unpublished Research in Progress, Ohio State University 1987.
23. A. C. Roberts and A. H. Cottrell: *Phil. Mag.*, 1956, vol. 1, p. 711.
24. G. W. Greenwood and R. H. Johnson: *Proc. Roy. Soc. A*, 1965, vol. 283, pp. 403-422.
25. S. F. Pugh: *J. Inst Met.*, 1957, vol. 86, pp.497-503.

F. Creep Resistant Materials

Theoretically, the understanding of creep in pure metals is still not complete. In most commercially interesting systems, the situation is still more complicated. In examining these materials from a mechanical-behavior point of view it is often found that creep resistant metals have: 1) unusually high stress exponents and 2) unusually high activation energies for creep. While these observations cannot be explained from first-principles theories, they can be rationalized somewhat by considering the structure of creep-resistant materials. These materials usually contain many phases, and high volume fractions of second phase. Thus, in considering creep the following must be considered:

How is mechanical continuity maintained across phases (i.e. what's deforming and where?)
What constitutive relations describe the interfaces (temperature and stress effects)?
What are the activation energies for creep of each phase?
How do dislocations cross inter-phase boundaries?
How do the relative proportions of each phase change with temperature?
What structural changes occur under stress and temperature?
Is the morphology which develops dependent on stress?
(There are other considerations, too).

Thus, quite alot of experimental and analytical work is required to develop an understanding of a single advanced system. Mechanics, mechanistics and interface issues must all be considered. However, much of the understanding gleaned from simpler systems can certainly be applied.